OAK RIDGE
NATIONAL LABORATORY

ORNL/TM-2001/289

MANAGED BY UT-BATTELLE
FOR THE DEPARTMENT OF ENERGY

Waste Preparation and Transport Chemistry: Results of the FY 2001 Studies

February 2002

R. D. Hunt
J. S. Lindner
A. J. Mattus
J. C. Schryver
C. F. Weber

UT-BATTELLE

ORNL-27 (4-00)

ORNL/TM-2001/289

Nuclear Science and Technology Division

Waste Preparation and Transport Chemistry: Results of the FY 2001 Studies

R. D. Hunt   J. C. Schryver[†]
J. S. Lindner*   C. F. Weber
A. J. Mattus

*Diagnostic Instrumentation and Analysis Laboratory, Mississippi State University
'Computing and Computational Sciences Division, ORNL

February 2002

CONTENTS

CONTENTS

LIST OF TABLES

LIST OF FIGURES

vii

INTRODUCTION

During FY 2001, tank farm operations at Hanford and the Savannah River Site (SRS) continued to be negatively impacted by the unintended formation of solids. At Hanford, the primary solids formation problem involves a series of plugged pipes and pumps during the saltwell pumping activities of the interim stabilization program. For example, transfers of tank S-102 waste were suspended due to a plugged pipeline or a mechanical problem with the transfer pump. The replacement pump then failed within 2 weeks.

In contrast, since full-scale waste remediation activities such as vitrification were initiated, the SRS has encountered a wider range of problems due to unwanted solids. The 2H evaporator system was shut down because of the formation of aluminosilicate deposits with enriched uranium in the evaporator pot. While high concentrations of aluminum are expected in the tank waste due to previous canyon operations, the primary source of silicon is the recycle stream from the vitrifier. While solids formation can be expected when waste streams are combined, the formation of the aluminosilicate deposits required an elevated temperature within the evaporator. The shutdown of the 2H evaporator led to a severe shortage of tank space. Therefore, the SRS tank farm was forced to transfer highly concentrated waste, which led to a plugged transfer pump in tank 32. For each of the proposed cesium removal technologies for the SRS, unwanted solids formation occurred during the large laboratory-scale tests prior to the final selection of the solvent extraction process. It can be expected that further problems will be encountered as more unit operations of the remediation effort are deployed and as more waste streams are combined. Since these problems have already led to costly schedule delays, the tank farm operators at both sites have identified the prevention of solids formation as a high-priority need.

In response to this need, the Tank Focus Area has assembled a team of researchers of researchers from AEA Technology, Florida International University (FIU), Fluor Hanford, Mississippi State University (MSU), Oak Ridge National Laboratory (ORNL), and Savannah River Technology Center (SRTC) to evaluate various aspects of the waste preparation and transport chemistry. The majority of this effort was focused on saltcake dissolution and saltwell

pumping. The results of the AEA Technology, FIU, and MSU studies of saltcake dissolution and slurry transfers for Hanford are discussed in detail in a companion report prepared by T. D. Welch in 2001 (ORNL/TM–2001/197). Staff members at Fluor Hanford have continued to conduct saltcake dissolution tests on actual tank waste (documented in reports prepared by D. L. Herting in 2000 and 2001). It should be noted that full-scale saltcake dissolution at Hanford is scheduled to begin in FY 2002. While the Hanford effort is focused on the transfer of waste from one tank to another, the objective of the SRTC study is the formation of aluminosilicates at elevated temperatures, which are present in the waste evaporator.

The ORNL effort is addressing problems of solids formation at Hanford and the SRS. At Hanford, nearly all of the pipeline plugs have been caused by sodium phosphate needle crystals. ORNL determined problematic concentrations of phosphate and fluoride, which can lead to additional pipeline plugs. Fluoride concentration is an important factor since sodium phosphate and sodium fluoride can combine to form natrophosphate, which is potato shaped and less likely to form a plug. A series of viscosity tests has been performed on key components in the Hanford waste. The viscosity results have been used to determine other key factors in potential plug formation and to develop an artificial neural network, which can predict the highest possible viscosity for thermodynamically unstable chemical systems at Hanford. With the assistance of MSU, ORNL researchers have studied the effects of Ostwald ripening and carbon dioxide on sodium phosphate crystals. With Ostwald ripening, many small sodium phosphate crystals are converted into a few large sodium phosphate crystals. After 3 to 4 days, the viscosity of the resulting solution is significantly lower than that of the initial solution. Therefore, a sodium phosphate plug may be more easiiy removed after a few days. The use of carbon dioxide to remove sodium phosphate plugs has also been evaluated. The addition of carbon dioxide will lower the pH of the solution, which will also increase its temperature. The solubility of sodium phosphate increases as the temperature increases and as the hydroxide concentration decreases.

The ORNL effort for the SRS was focused primarily on the formation and dissolution of the aluminosilicate in the 2H evaporator. The minimum temperature for the formation of hard deposits with a simple simulant was 50–60°C, which is in between the temperature of the waste in the evaporator feed tank and that in the evaporator. The hard deposits were much more likely

to form if the molar ratio of aluminum to silicon was close to 1. Simulant tests confirmed that 1.5 M nitric acid at 90°C could be used to remove the deposits from the evaporator pot. However, high-pressure water was needed to remove the. deposits from the transfer lines. The simulant tests also indicated that a silicon gel was likely to form in the evaporator pot, and gel was observed during the actual remediation effort. Since additional aluminosilicate deposits are likely, potential low-temperature alternatives to the 1.5 M nitric acid process were evaluated. The dissolution results indicated that acetic acid solution, citric acid, and maleic acid are promising alternatives. Other findings for the SRS and Hanford are presented in the following section. The material is presented as bulleted items so the key points can be more readily comprehended.

KEY POINTS

More Transfer and Processing Problems to Come

- Saltwell pumping efforts at Hanford continue to result in plugged transfer lines.
- Unwanted solid formation at the SRS has resulted from to a critical shortage of tank storage space.
  - Blending of tank waste (aluminum rich) with a secondary waste stream from the vitrifier (silicon rich).
  - Transfer of more-concentrated supematants.
- Savannah River has encountered unwanted solids formation with its cesium removal technologies.
- Transfer problems are expected to increase in number and variety as more unit operations for the full-scale remediation effort are tested and deployed.

High Viscosity Sodium Phosphate Solids at Hanford

- Key factors in the formation of high-viscosity sodium phosphate solids at Hanford are as follows:

    - Temperature (25–20°C better than 30–25°C for high-viscosity solids).

    - Rate of cooling (faster for high-viscosity solids).

    - Initial ionic strength (intermediate values better for high-viscosity solids).

    - Phosphate concentration (higher concentration-better for high-viscosity solids).

        - Sodium phosphate needle crystals-straw-like.

    - Fluoride concentration (higher concentration-worse for high-viscosity solids).

        - Natrophosphate (sodium phosphate-sodium fluoride double salt)-potato shaped.

    - Sulfate concentration (higher concentration-worse for high-viscosity solids).

        - Possible formation of a competing double salt.

- Potentially problematic concentrations of phosphate and fluoride were identified.

- Due to Ostwald ripening, the viscosity or stability of high-viscosity sodium phosphate solids drops dramatically between the third and fourth days.

- Experimental results and model predictions clearly indicate that the addition of carbon dioxide, which will react with water to form carbonic acid, can attack the sodium phosphate through two distinct mechanisms.

    - Solubility of sodium phosphate increases as the sodium hydroxide concentration decreases.

        Solubility of sodium phosphate increases as the temperature of the solution increases.

- The ability of the artificial neural network to predict the highest viscosity for thermodynamically unstable chemical systems at Hanford has improved significantly.

Aluminosilicate Deposits and Sodium Nitrate Plug at Savannah River

- In simulant tests, nitric acid could remove the aluminosilicate deposits .in the evaporator pot, but it was not effective for deposits in the lift line or the gravity drain.

- Acetic acid solution, citric acid, and maleic acid are potential low-temperature alternatives for the removal of sodalite deposits at the SRS.

- During the nitric acid dissolution of aluminosilicates, the available surface area is a key variable in the formation of a silica gel.

  - No gel with fine powder.

  - Gel with a single piece (same weight as the fine powder).

- The minimum temperature for the formation of aluminosilicate deposits with a simple SRS simulant **is** in the range of 50 to 60°C, which is in between the temperature of the waste in the evaporator feed tank and that in the evaporator.

- At SRS, the transfer of supernatant, which had an initial specific gravity of 1.48 g/mL and temperature of 57 °C, led to a nitrate plug in a transfer pump.
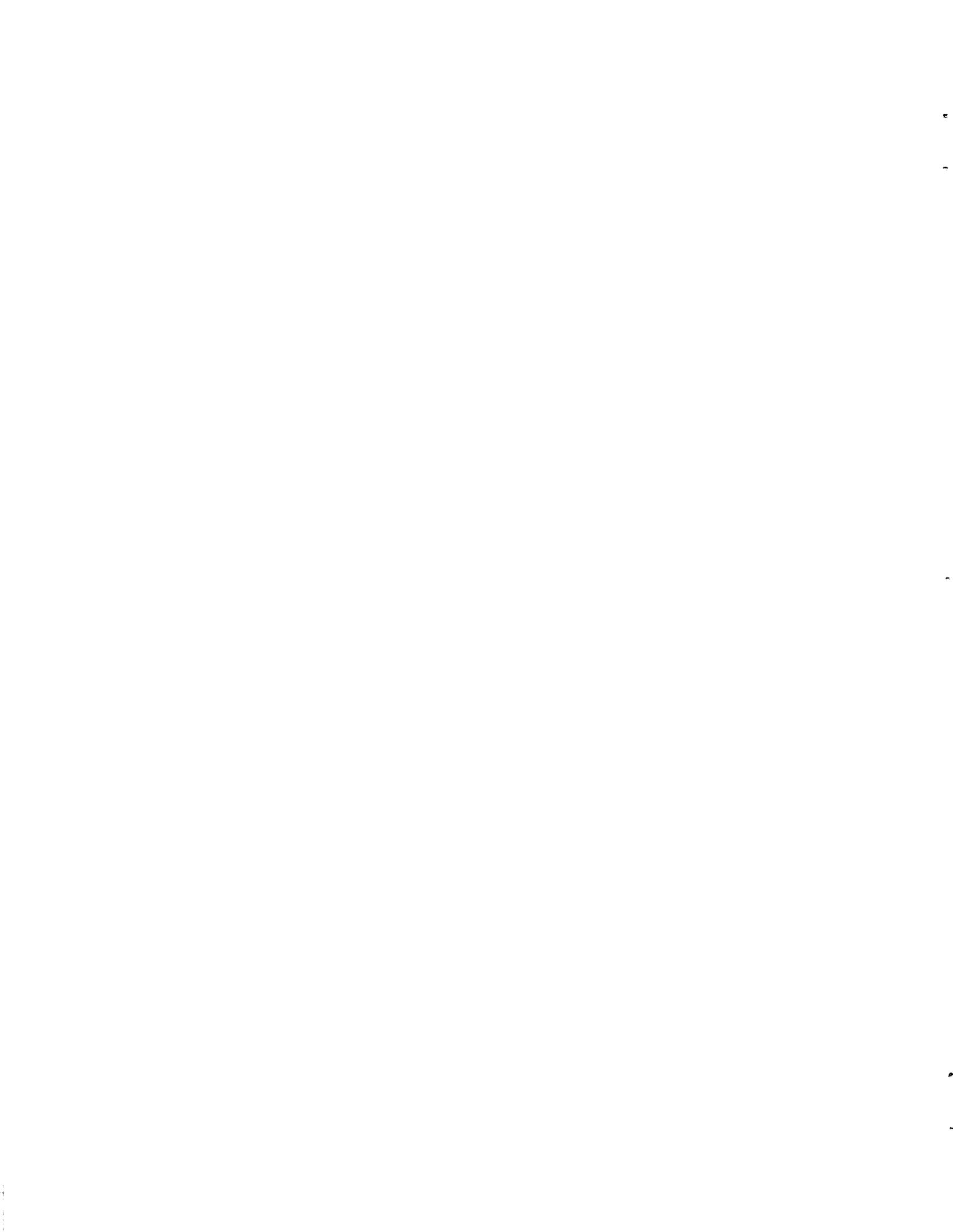
1. INTRODUCTION

The remediation plans for the nuclear wastes stored at Hanford, and the Savannah River Site (SRS) assume that the supematants can be successfully transferred from one tank to another or to a treatment facility and that filtered liquid can be easily passed through unit operations at a process facility. While the transfer of dilute-liquids would not likely be problematic, limited tank space has forced the tank farm operators to concentrate these supematants to levels close to saturation. Supematant transfers at Hanford and the SRS have clearly demonstrated that the transfer of these supematants can easily lead to plugged pipelines and pumps.

1.1 PLUGS DURING WASTE TRANSFERS AT HANFORD

At Hanford, the interim stabilization program is reducing levels of supematants and interstitial liquids in its single-shell tanks through its saltwell pumping activities. This effort has encountered problems with solids formation, which have led to a series of plugged pipes. In 2000, the transfer of 50,000 gal of filtered supematant from tank U-103 was suspended for several weeks due to a plug in the 02-A flex jumper. In an effort to avoid further plugs, the modifications such as larger flex jumpers and additional heating tracing were made to the transfer system. During tests on actual waste from tank U-103 (Herting, 1999), sodium phosphate was observed at temperatures as high as 20°C after a 50% dilution with water.

Past and present tests at Oak Ridge National Laboratory (ORNL) and Mississippi State University (MSU) assume that the formation of high-viscosity solids is the precursor to the formation of a sodium phosphate plug. In addition, the Hanford tank farm is currently planning to transfer only waste with a viscosity of 20 cP or less. During FY 2000, this effort (Hunt et al., 2000a) tried unsuccessfully to simulate the tank U-103 plug using the Best-Basis Inventory (BBI). However, high viscosity solids could be formed with a slight modification to the simulant formulation when the sample was cooled to 20°C. With this modified simulant formulation, the transition from low- to high-viscosity solids occurred as the phosphate concentration was increased from 0.04 M to 0.06 M and as the temperature was reduced from 30 to 20°C. Since the temperature of the waste in tank U-103 was approximately 30°C, the plug probably occurred when the waste in pipeline cooled slightly. Tests at Oak Ridge (Hunt et al., 2000a) and MSU

(Toghiani and Lindner, 2001) confirmed that the sodium phosphate is the key solid in the formation of the tank U-103 plug. An earlier study (Hunt et al., 1999) had also indicated that the pipeline plug due to waste from tank SX-104 was most likely caused by sodium phosphate. It should be possible to avoid transfer problems with sodium phosphate if the following precautions are followed (Herting, 1999). First, the tank waste should not be heated prior to the transfer. Second, the waste should not be allowed to cool during the transfer. Third, the waste should be kept moving during the transfer.

Problems with waste transfers have continued into 2001. Transfers of tank S-102 waste were suspended due to a plugged pipeline or a mechanical problem with the transfer pump. The replacement pump failed within 2 weeks. Information from the BBI and the waste tank summary report table indicates that the phosphate and fluoride concentrations prior to any dilution are 0.56 and 0.047 M, respectively. A preliminary analysis of the tank S-102 waste indicates that a sodium phosphate plug is a likely cause. This transport difficulty has adverse impacts on worker safety as well as remediation costs and schedule. Unless the movement of equipment in a waste tank can be performed remotely, then tank farm operators can expect that their workers will receive exposure to radiation. The increases in remediation costs can be attributed to the acquisition of a new pump or line and the disposal of the contaminated equipment.

1.2 PLUGS DURING WASTE TRANSPORT AND TREATMENT AT SAVANNAH RIVER

1.2.1 Evaporator Systems

The tank farm operators at **the** SRS are encountering a wider range of problems as a result of unwanted solids since the initiation of full-scale waste remediation activities such as vitrification. The dilute recycle stream from its vitrifier, which is called the Defense Waste Processing Facility (DWPF), continues to be sent to the tank farm for evaporation and storage. Due to limited tank space, this silicon-rich waste has been combined with an aluminum-rich waste stream from canyon operations in tanks 38H and 43H. This combined waste was processed through the 2H evaporator, which reduced the volume of aluminum-rich waste by

2

2530% and the volume of the recycle stream by 90%. Unfortunately, the operating temperature of the evaporator produced sodium aluminosilicate solids, which adversely affected the performance of the evaporator. In 1997, the gravity drain line from the 2H evaporator became plugged with sodium aluminosilicate and sodium diuranate. At this time, the sodium diuranate did not pose a criticality concern. In 1999, the evaporator operations were suspended because of poor performance. A subsequent inspection showed that solids were present on all exposed interior surfaces of the evaporator. The evaporator was shut down because the amount of ^{235}U in these evaporator deposits was a criticality concern. In 2001, two distinctly different methods were used to remove the deposits in the 2H evaporator system (Boley et al., 2000). Operators used 1.5 M nitric acid at 90°C to remove the deposits from the pot of the evaporator system, while a high-pressure water jet was used to clear the plugged lift line. This same high-pressure process was used to clear the gravity drain line in 1997. It is important to note that high-aluminum and high-silicon waste streams are still stored in tanks 38H and 43H and be must evaporated. Therefore, additional problems with solids formation can be expected if the operating conditions are not modified.

Unwanted solids formation has also disrupted operations of the 3H evaporator. In 2001, waste from tank 32 could not be transferred to the 3H evaporator. The transfer line to the 3H evaporator is 400 ft long with a diameter of 2 in. An analysis of the tank 32 supernatant indicated that the plug was probably due to sodium nitrate, which **is** soluble in water. It should be noted that the 3H evaporator system has not received waste from the DWPF. In an effort to remove the sodium nitrate plug, the SRS tank farm personnel pressurized the transfer line to approximately 340 psig. However, the pressure did not dissolve the plug. After the location of the plug was determined to be the discharge iine of the feed pump, cold water and then hot water were used to remove the plug as anticipated. As available tank space at the SRS becomes more limited and the waste becomes more concentrated, then similar plugs can anticipated.

1.2.2 Cesium Removal Technologies

In addition to problems with waste transfers, each of the proposed cesium removal technologies for Savannah River has encountered process difficulties due to unwanted solids. At

Argonne National Laboratory, a long-term test of the caustic-side solvent extraction process, which was selected as the primary cesium removal technology, was stopped because attempts to reduce the pH of the aqueous strip effluent stream were not successful (Leonard et al., 2001). An inspection of the equipment indicated that more solids were formed in the extraction stages than in the scrub stages. These solids were on the inside wall of the rotors, while the mixing zone of the contactor was free of solids. An elemental analysis of the solids indicated the presence of sodium, aluminum, and sulfur. The solids were crystalline and contained many components, as indicated by on an X-ray diffraction spectrum. The main compounds were sodium nitrate, a sodium aluminosilicate, sodium sulfate, and aluminum sulfate pentahydrate. Other possible compounds include sodium chloride and natroalunite.

Another cesium removal technology that was evaluated during the past few years for the SRS is the Small-Tank Tetraphenylborate Process (STTP). This process uses sodium tetraphenylborate to precipitate and remove radioactive cesium from the waste and monosodium titanate to sorb and remove radioactive strontium and actinides. ORNL has demonstrated this process at the 1:4000 scale using a 20-L-capacity continuous-stirred tank reactor system (Lee and Collins, 2001). The final test was terminated 60 h earlier due to the failure of the fluid seals on the progressive-cavity pump for the slurry concentration system. The failure occurred while the third batch of slurry was being processed. While the STTP is designed to generate solids, the problem with the pump was most likely caused by palladium, which was already a solid in the initial catalyst feed. In addition to the failed seals, hydraulic performance occasionally indicated fluid flow problems in the pipes between the reactors and the various feeds.

The final cesium removal technology that was under consideration for the SRS was crystalline silicotitanate (CST), which is an ion exchanger. During small-column tests at ORNL, the whole bed of CST clumped together and could not be moved with shaking after 3 months of operations (Taylor and Mattus, 2001). Even though the column with clumped CST continued to operate normally, the clumped CST had to be forcibly removed with a thin metal rod. Tests at Sandia National Laboratories (Nyman et al., 2001) have shown that cancrinite will form on CST particles during storage in supernatant simulants for the SRS. At ORNL, a tall-column system was built to evaluate the flow-through hydraulic characteristics of CST (Welch et al., 2000) and

to test gas-disengaging equipment (Spencer et al., 2001). The test system consists of a 3-in.-diam, 20-ft-tall column with a 16-ft bed height. At the conclusion of the gas disengaging tests, the CST column had become frozen, and attempts to remove the CST with air pressure and a flexible metal coil were not successful. If CST is to be used in the SRS remediation effort, it must be further demonstrated that the CST can be slurried in and out of the ion-exchange column.

2. EXPERIMENTAL STUDIES ON SODIUM PHOSPHATE PLUGS FOR HANFORD

2.1 CHEMICAL COMPOSITIONS OF THE SIMULANTS FOR HANFORD

The FY 1999 samples (Hunt et al., 1999) were designed to determine the significance of aluminum, fluoride, hydroxide, nitrate, phosphate, silicate, and sulfate in the formation of high-viscosity solids for Hanford. The BBIs of the Hanford tanks were analyzed to determine reasonable high and low concentrations for each of the seven components. Nearly all of these concentrations were reduced by a factor of 2 in order to produce samples with reasonable specific gravities, which can be as high as 1.4 g/mL. In the FY 2000 tests (Hunt et al., 2000a), carbonate was added to some of the Hanford formulations because the stability of the high-viscosity solids increased with the addition of sodium carbonate. The high and low concentrations of the key components in the FY 2001 samples are given in Table 1. Aluminum nitrate, sodium carbonate, sodium fluoride, sodium hydroxide, sodium nitrate, sodium phosphate, sodium silicate, sodium sulfate, and deionized water were used in the sample preparation. The composition of each sample is provided in Table 2. The specific gravity of the FY 2001 samples ranged from 1.1 to 1.4 g/mL.

Table 1. High and low concentrations of the components in FY 2001 viscosity samples

Concentration level	Concentration (mol/L) by component							
	$Al(OH)_4^-$	CO_3^{2-}	F	OH^-	NO_3^-	PO_4^{3-}	SiO_2	SO_4^{2-}
High	0.5	0.3	0.4	4.0	4.0	0.5	0.125	0.125
Low	0.1	0.01	0.01	1.0	1.0	0.025	0.025	0.025

Table 2. Concentrations of the components in FY 2001 viscosity samples

Sample ID	Concentration (mol/L) by Component							
	$Al(OH)_4$	CO_3^{2-}	F^-	OH^-	NO_3	PO_4^{3-}	SiO_2	SO_4^{2-}
D1	0.5	0.3	0.20	2.5	2.5	0.5	0.125	0.125
D2	0.5	0.3	0.22	2.5	2.5	0.5	0.125	0.125
D3	0.5	0.3	0.25	2.5	2.5	0.5	0.125	0.125
D4	0.5	0.3	0.29	2.5	2.5	0.5	0.125	0.125
D5	0.5	0.3	0.33	2.5	2.5	0.5	0.125	0.125
D6	0.5	0.3	0.40	2.5	2.5	0.5	0.125	0.125
D7	0.5	0.3	0.16	2.5	2.5	0.4	0.125	0.125
D8	0.5	0.3	0.18	2.5	2.5	0.4	0.125	0.125
D9	0.5	0.3	0.20	2.5	2.5	0.4	0.125	0.125
D10	0.5	0.3	0.23	2.5	2.5	0.4	0.125	0.125
D11	0.5	0.3	0.27	2.5	2.5	0.4	0.125	0.125
D12	0.5	0.3	0.32	2.5	2.5	0.4	0.125	0.125
E1	0.1	0.3	0.05	4.0	1.0	0.4	0.025	0.025
E2	0.1	0.3	0.05	3.0	2.0	0.4	0.025	0.025
E3	0.1	0.3	0.05	2.0	3.0	0.4	0.025	0.025
E4	0.1	0.3	0.05	1.0	4.0	0.4	0.025	0.025
E5	0.1	0.3	0.1	4.0	1.0	0.4	0.025	0.025
E6	0.1	0.3	0.1	3.0	2.0	0.4	0.025	0.025
E7	0.1	0.3	0.1	2.0	3.0	0.4	0.025	0.025
E8	0.1	0.3	0.1	1.0	4.0	0.4	0.025	0.025
E9	0.1	0.3	0.05	4.0	1.0	0.3	0.025	0.025
E10	0.1	0.3	0.05	3.0	2.0	0.3	0.025	0.025
E11	0.1	0.3	0.05	2.0	3.0	0.3	0.025	0.025
E12	0.1	0.3	0.05	1.0	4.0	0.3	0.025	0.025
E13	0.1	0.3	0.05	4.0	1.0	0.2	0.025	0.025
E14	0.1	0.3	0.05	3.0	2.0	0.2	0.025	0.025
E15	0.1	0.3	0.05	2.0	3.0	0.2	0.025	0.025
E16	0.1	0.3	0.05	1.0	4.0	0.2	0.025	0.025
F1	0.1	0.01	0.01	4.0	1.0	0.1	0.025	0.025
F2	0.1	0.01	0.01	3.0	2.0	0.1	0.025	0.025
F3	0.1	0.01	0.01	2.0	3.0	0.1	0.025	0.025
F4	0.1	0.01	0.01	1.0	4.0	0.1	0.025	0.025
F5	0.1	0.01	0.01	1.0	1.0	0.025	0.025	0.25
F6	0.1	0.01	0.3	1.0	1.0	0.025	0.025	0.25
F7	0.1	0.3	0.01	1.0	1.0	0.025	0.025	0.25
F8	0.1	0.3	0.01	1.0	1.0	0.025	0.025	0.025
F9	0.1	0.01	0.3	1.0	1.0	0.025	0.025	0.025
F10	0.1	0.3	0.3	1.0	1.0	0.025	0.025	0.025
F11	0.5	0.3	0.17	2.5	2.5	0.5	0.125	0.125
F12	0.5	0.3	0.13	2.5	2.5	0.4	0.125	0.125
F13	0.1	0.3	0.15	3.0	2.0	0.4	0.025	0.025
F14	0.1	0.3	0.1	3.0	2.0	0.3	0.025	0.025
F15	0.1	0.3	0.15	3.0	2.0	0.3	0.025	0.025
F16	0.1	0.3	0.1	3.0	2.0	0.2	0.025	0.025

2.2 FORMATION AND STABILITY OF SODIUM PHOSPHATE PLUGS

Most of the FY 2001 tests were focused on the formation of sodium phosphate and natrophosphate, which are needle-like and potato shaped, respectively. As shown in Eq. (1), the conversion of sodium phosphate to natrophosphate, which is sodium phosphate-sodium fluoride double salt, reduces the potential for high-viscosity solids:

$$2Na_3PO_4 \text{ (needle-like)} + NaF + 19H_2O \rightarrow Na_7(PO_4)_2F \cdot 19H_2O \text{ (potato shaped)} . \quad (1)$$

The viscosity tests were designed to simulate two distinctly different waste transfer scenarios. The first scenario involves a slight temperature reduction during the transfer. The River Protection Project (RPP) at Hanford has set 50°C as the minimum temperature for its cross-site transfers. During a cross-site transfer, the temperature of the waste is expected to drop by a maximum of 5°C. During a saltwell pumping, RPP staff members add water at ambient temperature to the tank waste and normally transfer the diluted waste to a nearby tank. The temperature of the diluted waste is not controlled. However, the temperature drop during the transfer should be relatively small if the transfer time based on transfer distance and flow rate is reasonably short. The second scenario, which involves a significant drop in temperature within a few hours, would occur if a transfer pump failed. Similar effects would be observed if a transfer system is not rinsed shortly after a transfer. The results of these viscosity tests were used in conjunction with earlier results to further refine a neural network, which predicts the maximum viscosity of a Hanford waste based solely on its chemical composition. It should be noted that the Hanford simulants can produce solids that are not thermodynamically stable. Therefore, the neural network predictions can be different from the viscosity calculations of an equilibrium model such as the Environmental Simulation Program (ESP).

Even though our understanding of the behavior of sodium phosphate has increased significantly, further sodium phosphate plugs can be expected. When the RRP encounters a pipeline plug during its saltwell pumping activities, the standard operating procedure involves the immediate application of high-pressure water to the blockage. This plug removal method is clearly the most cost- and time-effective procedure if the plug can be removed quickly. However, the continued application of high-pressure water may actually increase the stability of

the plug. In a static system, sodium phosphate can form high-viscosity solids when the temperature is lowered to approximately 27°C. The high-viscosity sodium phosphate solids are more likely to occur when the temperature of the sample is reduced rapidly. The final objectives of the Hanford effort were to determine the effects of Ostwald ripening and/or carbon dioxide on the stability of the high-viscosity sodium phosphate solids.

In previous years, this effort (Hunt et al., 2000a) had developed simulated pipeline plugs for the annual environmental design contest of the Waste-Management Educational and Research Consortium. Unfortunately, sodium phosphate-based plugs would weaken with time, which hampered the evaluation of plug removal technologies. This weakening could be due to the adsorption and subsequent reaction of carbon dioxide or to Ostwald ripening. Sealed samples of the plug formulations indicated that the samples were susceptible to Ostwald ripening, as shown in Eq. (2):

$$\text{many small crystals} \rightarrow \text{time (Ostwald ripening)} \rightarrow \text{few large crystals} . \qquad (2)$$
$$\text{(kinetically favored)} \qquad\qquad\qquad \text{(thermodynamically favored)}$$
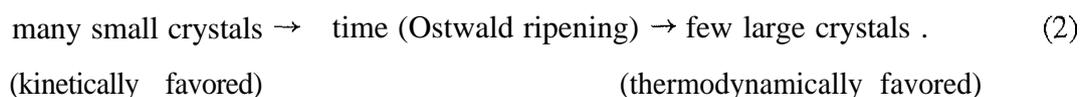
The formation of small crystals in the plug is kinetically favored over larger crystals since it is easier to nucleate many small crystals than a few large crystals. However, larger crystals should be thermodynamically favored. It has been demonstrated that many small sodium phosphate crystals are formed initially and that these small crystals slowly grow into a few large sodium phosphate crystals. This process, where the smaller crystals act as building blocks for the larger crystals, is known as Ostwald ripening (Boistelle and Astier, 1988). This normally spontaneous event does not always occur.

2.2.1 Viscosity Measurements During Gradual Waste Cooling

After the 20-mL samples in Table 2 were prepared, they were placed in an Aquatherm water bath shaker. After the samples were maintained at 80°C for the first week, the temperature of the samples was lowered to 65 °C for the second week. During the third week, the samples were permitted to equilibrate at 50°C prior to the initial viscosity measurements. While the samples were in the water bath shaker, they were rotated at a rate of 100 rpm. However, the

rotation did not prevent any solids from settling to the bottom of the bottle. Prior to each viscosity measurement, the height of the settled solids was measured. Each sample was then shaken by hand to resuspend all of the solids in the sample before 16 mL of the sample was transferred into the preheated small sample adapter for the Brookfield DV-III rheometer. The volume below the spindle in the small sample adapter is 2.6 mL, which is 16% of the total sample volume. Because solids settled into this void space during most of the viscosity tests, the viscosity measurements should be considered minimum values. The sample was then permitted to equilibrate for 15 min. For each sample, two viscosity tests were performed in an effort to determine the effects of shear rate and time. In the first test, the shear rate was varied from 12 to 122 to 12 s^{-1}. The particular shear rate was maintained for a period of 2 min before it was increased or decreased by 12 s^{-1}. In the other test, a shear rate of 61 s^{-1} was normally applied to the sample for 5 min. If high-viscosity solids were observed, then a lower shear rate as indicated was used. The viscosity results from the 5-min tests are presented in Table 3. The height measurement of the gravity-settled solids was converted to the volume percent, which is given in Table 4. At the end of the 50°C tests, the samples were allowed to equilibrate at 45 °C for 3.5 days prior to next set of viscosity measurements. An equilibration period for the next lower temperature was maintained at a minimum of 3.5 days, and the temperature was reduced in increments of 5 °C until it reached 15°C.

2.2.2 Viscosity Measurements After a Simulated Pump Failure

After the gradual-cooling experiments were completed, the samples were again heated to 60°C for approximately 1 week. After the equilibration period, the height of the solids was measured, and 16 mL of the hot sample was transferred into the rheometer's small sample adapter, which was also heated to 60°C. The temperature of the water bath, which controls the temperature of the small sample adapter, was reduced to 30°C in an effort to simulate a pump failure. The initial rate of cooling was slightly more than 0.7 °C/m, and the cooldown period was approximately 2 h. After the sample was permitted to equilibrate for 1 h, two viscosity tests were performed in an effort to determine the effects of shear rate and time. The results are presented in Table 5.

Table 3. Viscosity of the FY 2001 samples during gradual waste cooling

Sample ID	Viscosity (cP) by temperature							
	50°C	45°C	40°C	35°C	30°C	25°C	20°C	15°C
D1	2.6	2.6	2.5	2.5	2.5	2.8	3.3	3.9
D2	2.6	2.7	3.2	2.5	3.5	4.0	4.6	5.3
D3	2.5	2.7	3.1	2.5	3.0	3.4	4.0	5.1
D4	2.4	2.6	2.5	2.5	2.8	3.1	3.6	4.4
D5	2.4	2.6	2.8	2.5	2.4	2.8	3.2	3.9
D6	2.5	2.7	2.7	2.5	2.9	3.4	3.9	4.8
D7	2.6	2.7	2.9	2.5	3.5	4.0	4.4	5.1
D8	2.5	2.6	3.0	2.5	3.3	3.7	5.1	5.9
D9	2.4	2.6	2.9	2.5	3.3	3.8	5.3	6.3
D10	2.4	2.7	2.8	2.5	3.2	3.8	4.5	5.4
D11	2.3	2.4	2.7	2.5	2.9	3.4	4.1	5.0
D12	2.3	2.4	2.6	2.5	3.0	3.5	4.1	5.0
E1	3.0	2.7	2.8	2.6	2.8	2.7	2.8	3.3
E2	2.3	2.2	2.4	2.5	2.8	2.9	3.2	3.8
E3	2.1	2.1	2.2	2.3	2.5	2.9	3.0	3.6
E4	2.3	2.3	2.2	2.3	2.6	3.1	3.1	3.4
E5	2.5	2.5	2.4	2.7	3.0	3.5	3.7	3.7
E6	2.3	2.2	2.2	2.5	2.7	3.4	3.6	4.2
E7	2.3	2.3	2.3	2.4	2.5	3.1	3.2	3.6
E8	2.0	2.0	2.1	2.3	2.3	2.6	2.8	3.3
E9	2.4	2.4	2.5	2.7	2.8	3.1	3.5	4.1
E10	2.1	2.2	2.3	2.5	2.7	3.2	3.5	4.1
E11	2.1	2.2	2.2	2.3	2.9	3.0	3.4	3.9
E12	2.0	2.0	1.9	2.1	2.4	3.0	3.4	3.8
E13	2.1	2.4	2.5	2.7	2.9	3.6	3.7	4.4
E14	2.1	2.2	2.3	2.4	2.6	3.2	3.3	3.7
E15	2.0	2.0	2.1	2.3	2.6	3.8	3.2	3.7
E16	1.8	2.0	2.1	2.4	2.5	2.8	3.0	3.5
F1	1.8	1.7	1.8	2.0	2.3	2.5	2.8	2.9
F2	1.6	1.6	1.7	1.8	2.2	2.5	2.7	2.8
F3	1.6	1.5	1.7	1.9	2.0	2.3	2.5	2.6
F4	1.4	1.4	1.6	1.7	1.8	1.9	2.1	2.2
F5	1.0	1.0	1.1	1.2	1.3	1.5	1.6	1.8
F6	1.0	1.1	1.2	1.3	1.5	1.5	1.7	2.0
F7	1.1	1.2	1.3	1.4	1.5	1.7	1.9	2.1
F8	1.0	1.1	1.2	1.3	1.4	1.6	1.7	1.9
F9	1.0	1.0	1.1	1.2	1.3	1.4	1.6	1.8
F10	1.1	1.1	1.2	1.3	1.5	1.5	1.7	2.0
F11	1.8	2.7	2.7	2.8	3.1	3.5	3.5	3.7
F12	2.6	2.6	2.7	2.8	2.9	3.1	3.3	3.7
F13	2.2	2.3	2.3	2.5	2.7	2.9	3.0	3.3
F14	2.0	2.3	2.2	2.3	2.6	2.9	3.2	3.5
F15	2.0	2.2	2.2	2.2	2.6	2.8	3.1	3.3
F16	1.9	2.1	2.1	2.2	2.5	2.8	2.9	3.1

Table 4. Volume of gravity-settled solids during gradual waste cooling

Sample ID	Volume percent by temperature							
	50°C	45°C	40°C	35°C	30°C	25°C	20°C	15°C
D1	25	20	20	20	15	15	15	15
D2	25	25	20	20	20	15	20	20
D3	25	20	20	20	20	20	20	20
D4	25	25	25	25	25	25	25	20
D5	25	25	25	20	25	20	20	20
D6	25	25	20	20	20	20	20	20
D7	20	15	15	15	20	20	20	20
D8	20	20	20	20	20	20	20	20
D9	20	20	15	15	20	20	15	15
D10	20	20	20	20	20	20	20	20
D11	20	25	25	20	20	20	20	20
D12	20	25	20	20	20	20	20	20
E1	10	25	25	25	20	20	20	25
E2	10	20	25	25	20	25	25	25
E3	10	20	20	20	15	25	25	25
E4	10	20	20	20	15	25	25	25
E5	10	20	20	30	25	25	25	25
E6	10	15	20	25	20	20	20	20
E7	10	15	20	20	20	20	20	20
E8	10	15	15	20	15	20	20	20
E9	10	20	20	20	20	20	25	20
E10	10	20	20	20	20	20	25	20
E11	10	15	20	20	25	25	25	25
E12	10	15	15	15	20	20	20	20
E13	5	5	10	15	20	20	20	20
E14	5	5	10	15	15	15	20	20
E15	5	5	5	10	10	10	15	15
E16	5	5	5	5	10	10	15	15
F1	<5	5	5	5	10	10	15	15
F2	5	5	5	5	5	5	10	15
F3	5	5	5	5	5	5	5	10
F4	5	5	5	5	5	5	5	5
F5	5	5	5	5	5	5	5	5
F6	5	5	5	5	5	5	5	5
F7	5	5	5	5	5	5	5	5
F8	5	5	5	5	5	5	5	5
F9	5	5	5	5	5	5	5	5
F10	5	5	5	5	5	5	5	5
F11	25	25	25	25	25	25	25	25
F12	15	15	15	20	20	20	25	25
F13	15	15	15	15	15	20	20	20
F14	15	15	15	15	15	15	20	20
F15	15	15	15	15	15	15	15	15
F16	10	10	10	10	10	10	15	15

Table 5. Simulated pump failure: initial volume of solids and final viscosity

Sample ID	Viscosity (cP): 60 to 30°C	Volume percent of solids: 60°C	Viscosity (cP): 50 to 20°C	Volume percent of solids: 50°C
D1	2.5	10	18[a]	15
D2	2.6	10	3.3	15
D3	2.6	10	3.1	15
D4	2.6	10	3.2	15
D5	2.6	10	3.0	20
D6	2.5	10	2.9	20
D7	2.5	10	3.0	15
D8	2.7	10	3.4	15
D9	2.7	10	3.1	15
D10	2.7	10	3.0	15
D11	2.6	10	3.2	20
D12	2.3	15	2.7	20
E1	150[a]	<5	4000[b]	10
E2	180[a]	5	1900[b]	10
E3	180[a]	<5	2400[b]	10
E4	200[a]	5	3700[b]	10
E5	160[a]	<5	1800[b]	10
E6	170[a]	5	3000[b]	10
E7	160[a]	5	1600[b]	10
E8	200[a]	5	2300[b]	10
E9	130[a]	5	1800[b]	10
E10	140[a]	5	1300[b]	10
E11	160[a]	<5	1300[b]	10
E12	130[a]	<5	1800[b]	10
E13	5.4	5	155[a]	5
E14	2.4	<5	175[a]	5
E15	3.6	<5	185[a]	5
E16	2.7	<5	3.2	5
F1	2.0	<5	2.6	<5
F2	1.9	<5	2.5	5
F3	1.9	<5	2.3	5
F4	1.6	<5	2.0	5
F5	1.4	5	1.6	5
F6	1.4	5	1.7	5
F7	1.6	5	2.0	5
F8	1.5	5	1.6	5
F9	1.4	<5	1.6	5
F10	1.4	5	1.9	5
F11	2.6	15	3.4	20
F12	2.7	15	3.4	15
F13	2.5	10	2.9	15
F14	2.6	10	3.9	10
F15	2.4	10	3.4	10
F16	2.2	5	2.9	5

[a]Shear rate of 1.2 s^{-1}.
[b]Shear rate of 0.12 s^{-1}.

Additional tests on simulated pump failure were performed at the minimum temperature for the cross-site transfers. The samples were heated at 50°C for 1 week. At the end of the , equilibration period, the volume percent of the gravity-settled solids was determined, and most of the hot sample was transferred into the rheometer's small sample adapter, which was also heated to 50°C. The temperature of the water bath, which controls the temperature of the small sample adapter, was reduced to 20°C. The initial rate of cooling was 0.5°C/m, and the cooldown took approximately 3 h. After the sample had reached 20°C, the viscosity measurements were made. For the simulated pump failures at 60 and 50°C, Table 5 shows the viscosity measurements obtained at a shear rate of 61 s^{-1} (unless noted otherwise) and the volume of settled solids at higher temperatures.

2.2.3 Effects of Gradual Waste Cooling and Simulated Pump Failure

While the primary purpose of the viscosity tests of gradual waste cooling and simulated pump failures was to provide additional data sets for the neural network, the viscosity results can also be used to make general observations about the formation of the high-viscosity sodium phosphate solids. First, the potential for high-viscosity solids increases as the rate of temperature cooling increases. In the gradual-cooling tests, high-viscosity solids were not observed in any of the FY 2001 samples. In sharp contrast, 15 samples produced high-viscosity solids after a rapid temperature loss during a pump failure simulation. Second, the viscosity of the high-viscosity solids in the simulated pump failure tests increased by an order of magnitude when the final temperature of sample was 20°C instead **of** 30 "C. Third, formation of high-viscosity sodium phosphate solids can be prevented if the fluoride concentration is sufficiently high. Potentially problematic fluoride concentrations with phosphate concentrations are presented in Table 6. It should be noted that an earlier sample with a phosphate concentration of 0.06 M and no fluoride produced high-viscosity solids when it was rapidly cooled to 20°C (Hunt et al., 2000a). Fourth, the primary contribution of sodium hydroxide and sodium nitrate is to the ionic strength of the samples. A previous study (Hunt et al., 2000a) demonstrated that the initial ionic strength of the simulant was a key factor in the formation of high-viscosity sodium phosphate solids. Under one set of test conditions, a sample with a low concentration of sodium hydroxide and a high

**Table 6. Potentially problematic phosphate concentrations
with respect to fluoride concentration**

Phosphate concentration (mol/L)	Safe fluoride concentration (mol/L)	Potentially unsafe fluoride concentration (mol/L)
0.5	> 0.2	< 0.2
0.4	> 0.13	< 0.1
0.3	> 0.1	< 0.05
0.2	> 0.1	< 0.05

concentration of sodium nitrate did not form high-viscosity solids while those with a higher concentration of sodium hydroxide and a lower concentration of sodium nitrate did generate high viscosity solids. Therefore, the sodium hydroxide concentration may be slightly more important than the sodium nitrate concentration. Fifth, inert solids such as sodium carbonate can increase the viscosity of the sodium phosphate solids. The inert solids serve the same role as mineral aggregates in concrete.

2.2.4 Effects of Ostwald Ripening

The effects of Ostwald ripening on high-viscosity sodium phosphate solids were examined. In the first test, the composition of the sample was 4 A4 hydroxide, 1 M nitrate, 0.5 M phosphate, 0.25 M sulfate, 0.1 A4 aluminate, 0.025 M silicon, and 0.01 M fluoride. Tests in **FY** 2000 (Hunt et al., 2000a) demonstrated that this composition would form a phosphate plug during both rapid and gradual cooling. The sample was heated to 50°C for 2 weeks, and the sample was then transferred to a Brookfield DV-III rheometer and cooled to 20°C in 2 h. The temperature of the sample was maintained at 20°C, and the sample was normally sealed to limit water losses to the atmosphere. The viscosity of the sample was periodically measured at a shear rate of 0.1 s^{-1}. The viscosity results are presented in Fig. 1. Initially, the low shear rate was needed to make the viscosity measurement. After 4 days, a higher shear rate could have been used in the viscosity measurement. However, higher shear rates were used only briefly to confirm that the viscosity of the sample was in excess of 20 cP. A shear rate of 0.1 s^{-1} was used to minimize the impact of the spinning cylinder in the rheometer on the Ostwald ripening. As

14
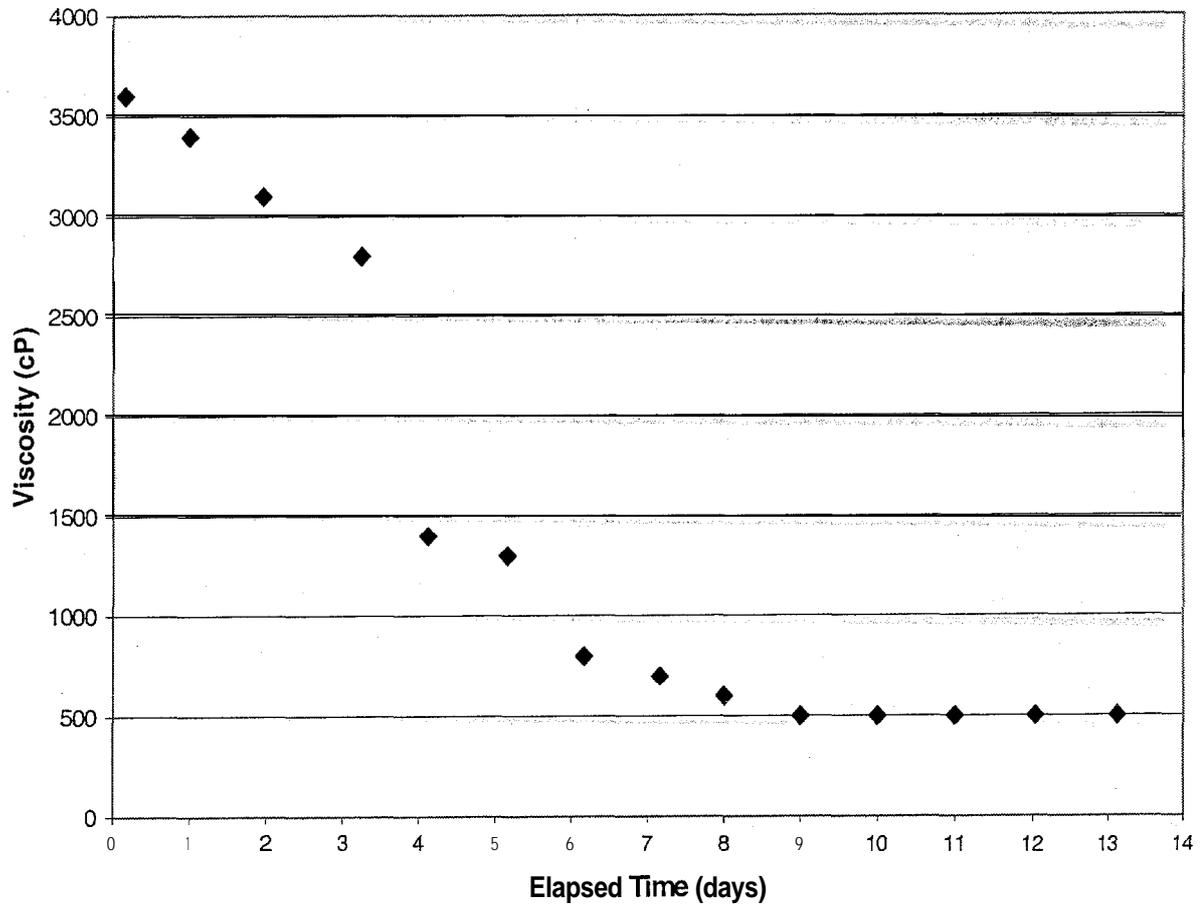
Fig. 1. Viscosity of the high-viscosity sodium phosphate solids as a function of time.

shown in Fig. 1, the viscosity of the sample decreased linearly for the first 3 days. A sharp drop was observed between the third and fourth days. The viscosity of the sample continued to drop until the viscosity reached 500 cP on the ninth day. No further changes in viscosity were observed through the 13th day.

During the tenth annual environmental design contest by the Waste-Management Educational and Research Consortium, several competing universities suggested that lower temperatures could facilitate the plug removal (Hunt et al., 2000a). The temperature of the sample was lowered to 10°C for 2 days. This lower temperature did not effect the viscosity of the sample. However, the lower temperature would probably increase the rate of Ostwald

ripening. On the 15th day, the temperature of the sample was increased to 30°C. After 1 day at 30°C, the viscosity of the sample was 18 cP at a shear rate of $0.1 \, s^{-1}$ and 3.3 cP at a shear rate of $61 \, s^{-1}$. These results clearly show that time, in addition to temperature, can be a key factor in the removal of the high-viscosity sodium phosphate solids.

2.2.5 Effects of Carbon Dioxide

During the tenth annual environmental design contest, the Purdue University and Montana Tech processes, which used a combination of carbon dioxide and applied pressure, appeared to be the most promising technologies for the removal of a sodium phosphate plug (Hunt et al., 2000a). A hot solution of 2 M sodium aluminate, 0.6 M sodium carbonate, 0.3 A4 sodium fluoride, 2 M sodium hydroxide, 8 M sodium nitrate, and 0.9 M sodium phosphate was cooled to form the sodium phosphate plug for the contest. The aluminate, phosphate, carbonate, and fluoride concentrations for the contest were considerably higher than the corresponding values for the supernatant in Hanford tank SX-104, which formed a sodium phosphate plug. A more accurate simulant of the tank SX-104 supematant was used in the following ESP projections. The carbon dioxide reacts with water to form carbonic acid. Since carbonic acid is considerably less dense than sodium hydroxide, the initial production of carbonic acid is used primarily to neutralize the caustic solution above the plug. At Purdue University, the minimum pH value that was achieved in the sodium phosphate was 5.7. The carbon dioxide and applied pressure removed approximately 70% of the plug by mass.

At MSU, a series of calculations using the ESP was performed to evaluate the effects of carbon dioxide additions to a sodium phosphate plug under adiabatic conditions. For this MSU study, the Hanford tank SX-104 simulant contained i M sodium aluminate, 0.1 M sodium carbonate, 0.3 M sodium fluoride, 2 M sodium hydroxide, 7 M sodium nitrate, and 0.3 M sodium phosphate. While the tank SX-104 simulant is clear at 50°C, a gel begins to form at 40°C. This gel is caused by sodium phosphate dodecahydrate. In the ESP simulations, 0 to 20 L of carbon dioxide was added to 1 L of the tank SX-104 surrogate at 37°C. The ESP model predicts that an increase in temperature will accompany the carbon dioxide addition. The sodium phosphate dodecahydrate was transformed to the sodium phosphate octahydrate form after the addition of

16

3 L of carbon dioxide. The temperature of this transition was 42°C. The temperature also corresponds to the approximate temperature for the octahydrate-to-dodecahydrate crystal transition. Therefore, an increase in plug temperature without the carbon dioxide addition would result in the same transition. The sodium phosphate solid would be completely dissolved if 4 L of carbon dioxide was added for each liter of tank SX-104 simulant. If the simulant temperature was reduced again, the sodium phosphate plug would then reappear. With the addition of 4 L of carbon dioxide, the solubility of the sodium aluminate decreased from 65 to 62 g/L, and a corresponding increase in gibbsite solids was predicted. The pH values of the tank SX-104 simulant before and after the addition of 4 L of carbon dioxide were 14.5 and 14.2, respectively. With the addition of 20 L of carbon dioxide per liter of simulant, the final pH would be 12.7, and 30 g of gibbsite would have precipitated.

These experimental results and model predictions clearly indicate that the carbon dioxide can attack the high-viscosity sodium phosphate solids through two distinct mechanisms. First, the solubility of sodium phosphate increases as the sodium hydroxide concentration decreases. This solubility trend would be expected based on the common ion effect. Second, the solubility of sodium phosphate increases as the temperature of the solution increases. For example, the average sodium phosphate solubility increased from 14 g/100 g of water at 25°C to 24 g/100 g of water at 40°C (Linke, 1965). These results were used to develop a thermodynamic model for the aqueous solutions of sodium phosphate (Weber et al., 1999). In conclusion, these results, in combination with the earlier observations on Ostwald ripening, indicate that hot water after a short delay may be the most effective method to remove the sodium phosphate plugs. If hot water cannot adequately reach the plug, then the addition of carbon dioxide is a reasonable, alternative.

3. VISCOSITY PREDICTIONS USING ARTIFICIAL NEURAL NETWORK MODELS

3.1 BACKGROUND

In FY 2000, this effort (Hunt et al., 2000a) attempted to predict peak viscosity based on the concentrations of aluminum, fluoride, hydroxide, nitrate, phosphate, silicate, and sulfate. Our

approach employs artificial neural network (ANN) models to capture nonlinearity in the relationships between compound concentrations and viscosity. Additional information on the ANN has been provided earlier (Hunt et al., 2000a). In FY 2000, the viscosity results were modeled with ANN ensembles using the adaptive boosting algorithm (ABA). This computationally intensive procedure was necessary due to the limited number of high-viscosity results. Individual ANN models trained on the original data set ignored high-viscosity values since they were so few in number, focusing instead on perfect prediction of the more numerous low-viscosity values. The ABA permitted the ensemble ANNs to learn to increase the weights on missed predictions of high-viscosity results. Therefore, the ANNs with the ABA were forced to focus more equally on the high- and low-viscosity results.

With the addition of sodium carbonate and several high-viscosity samples in FY 2001, viscosity results were again modeled with individual ANNs. The ANNs, which are nonlinear universal function approximators (Hornik et al., 1989), do not assume that the data come from any particular family of distributions such as a polynomial or an exponential. They can be used for prediction by learning an arbitrary nonlinear input-output mapping or for classification when each data point belongs to a single class such as high or low viscosity. A supervised learning paradigm incorporating feed-forward ANNs with a single hidden layer and nonlinear activation functions is often used for prediction where input-output mappings are nonlinear. The classical statistical technique for prediction is multiple linear regression. However, this technique is not recommended if the true relationship is nonlinear. Additional background can be found elsewhere (Bishop, 1995; Jain et al., 1996; Lippmann, 1987).

3.2 TRAINING AND VALIDATION METHODS

Any modeling effort should not merely fit an ANN model to a set of viscosity training data. With a sufficient number of nodes and weights, any sufficiently complex ANN model can provide an exact fit to a finite set of sample points. Unfortunately, a complex model often overfits the data and generalizes poorly to new samples that the model has not previously encountered. If the model cannot predict the previously untested sample composition, it would be of no value to the tank farm operators. Therefore, model performance was determined using

viscosity results that have been withheld from training or model development. When a data set is size limited, k-fold cross-validation is a data-efficient training procedure because every sample has an opportunity to serve as both training data for model development and test data for model validation.

The model has eight predictor compounds and a single output variable. Using k-fold cross-validation, the entire data set of 55 samples was divided into 11 randomly selected subsets, which were equal in size. Each subset contained a mixture of low- and high-viscosity samples. An independent ANN was trained using 10 of the 11 subsets, while the 11 th subset was used to estimate the generalization error of each model. The subset that was used to estimate error was rotated.

After several different candidate architectures were tested, a network with four hidden nodes was selected. Both input and output data were transformed using a nonlinear function into the $[0,1)$ interval. The predicted variable was defined as peak viscosity across the entire temperature range for the gradual waste cooling and for the simulated pump failures. Temperature was removed from the set of predictors because it was not a good indicator of viscosity of a specific sample. Figure 2, which contains one linear axis and one logarithmic axis, shows the nonlinear transformation of viscosity.

3.3 ANN PERFORMANCE

Results of ANN performance are given in transformed units. The range of mean squared error (MSE) in the test set from the 11 trained ANNs is shown in the first column of Table 7. It should be noted that the performance of the ANNs has continued to improve with each new set of viscosity results. The results from the final set of FY 2001 viscosity tests and an earlier viscosity study at Hanford (Kelly and Mauss, 1986) will soon be used to further improve the model. The architecture is designated by the notation 8x4x1, which indicates eight predictor variables (compounds), four hidden nodes, and a single output node (viscosity).

The median-performing ANN was selected for further analysis to avoid a biased test set. Because all of the viscosity results were used in the MSE evaluation, potentially problematic viscosity results must be in the data sets for the model development or the model validation. The

19
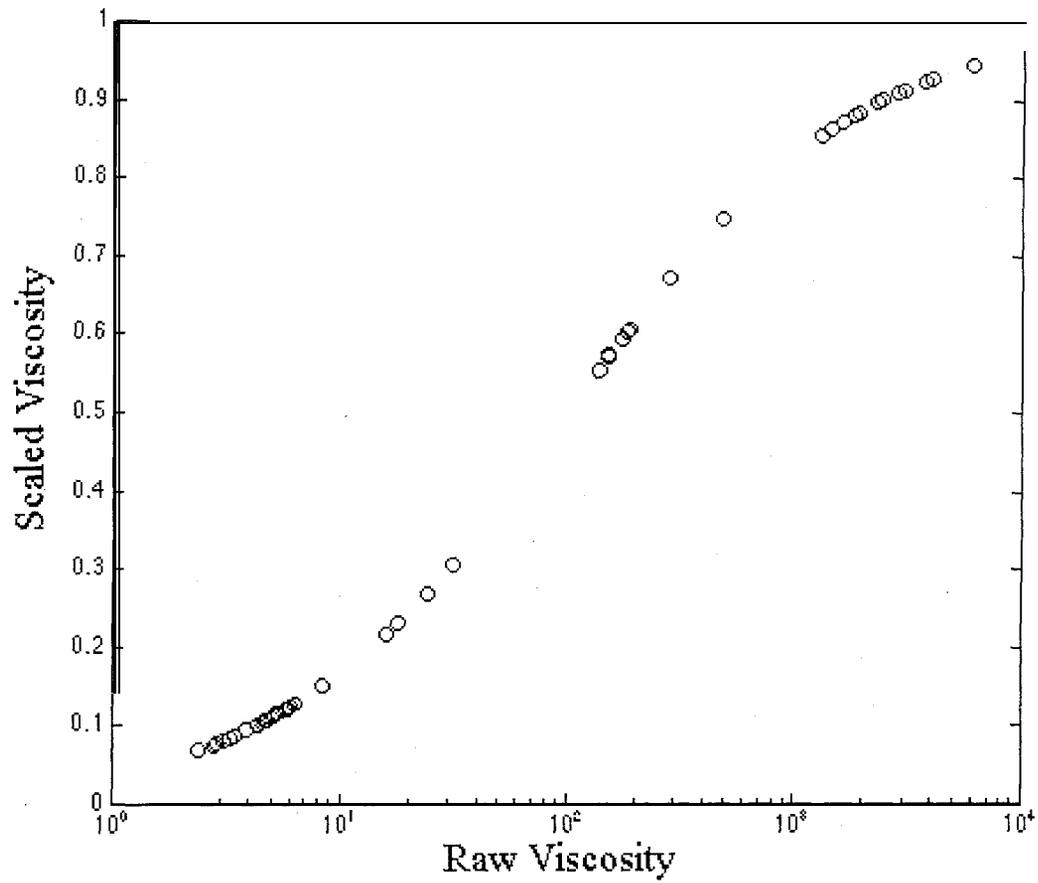
Fig. 2. Nonlinear transformation of viscosity into the [0,1) interval.

Table 7. Mean squared error (MSE) for artificial neural network (ANN) models

Performance of the ANN	MSE for the training data (model development)	MSE for the test data (model validation)
Best (1st)	0.0034	0.0008
Median (6th)	0.0029	0.0161
Worst (I lth)	0.0025	0.0814

selection of the median-performing ANN ensures that most problematic results should be in both, data sets. Previous attempts to model viscosity merely discriminated between two classes, which were high and low viscosity. Figure 3 shows that the median-performing ANN was able to predict raw viscosity values reasonably well. The dotted lines divide the scatter-plot in Fig. 3 into four quadrants. The upper right and lower left quadrants, respectively, are regions in which high- and low-viscosity samples are correctly classified. The upper left and lower right quadrants are regions representing incorrect classification. None of the samples were incorrectly classified, although a few low-viscosity points are marginally close to the predicted high-viscosity range.
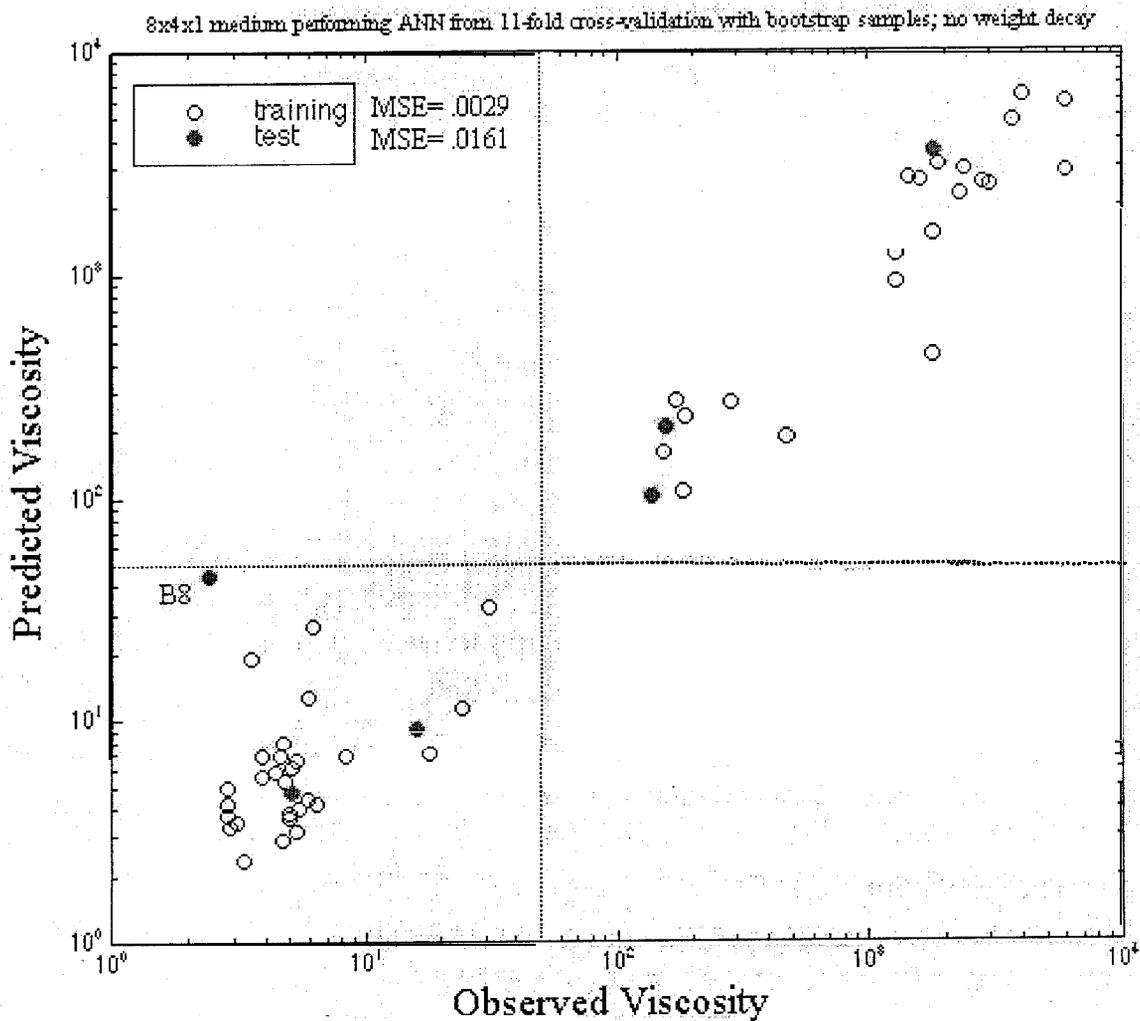

Fig. 3. Observed vs predicted viscosity for all samples.

21

Apart from the few low-viscosity results, all test samples are well within the range of predicted values in the training set. Inspection of Fig. 3 shows that qualitatively the median-performing ANN did a reasonable job of estimating raw viscosity values. These findings indicate that the predictability in the training set and the generalization capability are both good. These conditions are requirements that had to be satisfied before the Tank Focus Area would transfer this model to the Hanford tank farm.

An effort was made to determine the importance of each compound in the formation of high-viscosity solids. If this viscosity model was linear, then the global sensitivity can be estimated from the standardized beta coefficients in the linear model itself. Unfortunately, no corresponding method exists for ANNs. However, many researchers have computed local sensitivity values using Eq. (3), when all inputs (X_i) are not expressed in similar units across comparable ranges:

$$S_2(i) = \frac{X_i}{V} \cdot \frac{\partial V}{\partial X_i} .$$

(3)

As shown in Table 1, the concentrations of hydroxide and nitrate do not overlap with concentrations of the other key compounds. In Eq. (3), S_2 is a dimensionless index that adjusts for the scale of each X_i. In order to estimate a global sensitivity number from the set of local sensitivity scores, the following statistic was computed using Eq. (4):

$$Gs = \sum abs\left(S_2(i)\right) .$$

(4)

Absolute values were used in estimating global sensitivity (Gs) because magnitude, not direction, was the feature most critical to the importance of the predictor variable. The three most sensitive compounds were hydroxide, nitrate, and phosphate. An analysis of the Gs results indicated a bias toward compounds with higher concentrations.

Therefore, a slightly different approach was undertaken to minimize bias in the range of values for X_i. Scatter-plots of raw X_is vs raw viscosity were prepared as shown in Fig. 4. The solid line indicates smoothed model predictions obtained by varying a single predictor, while all of the other variables were held to their mean values. In some cases, a strong monotonic

22
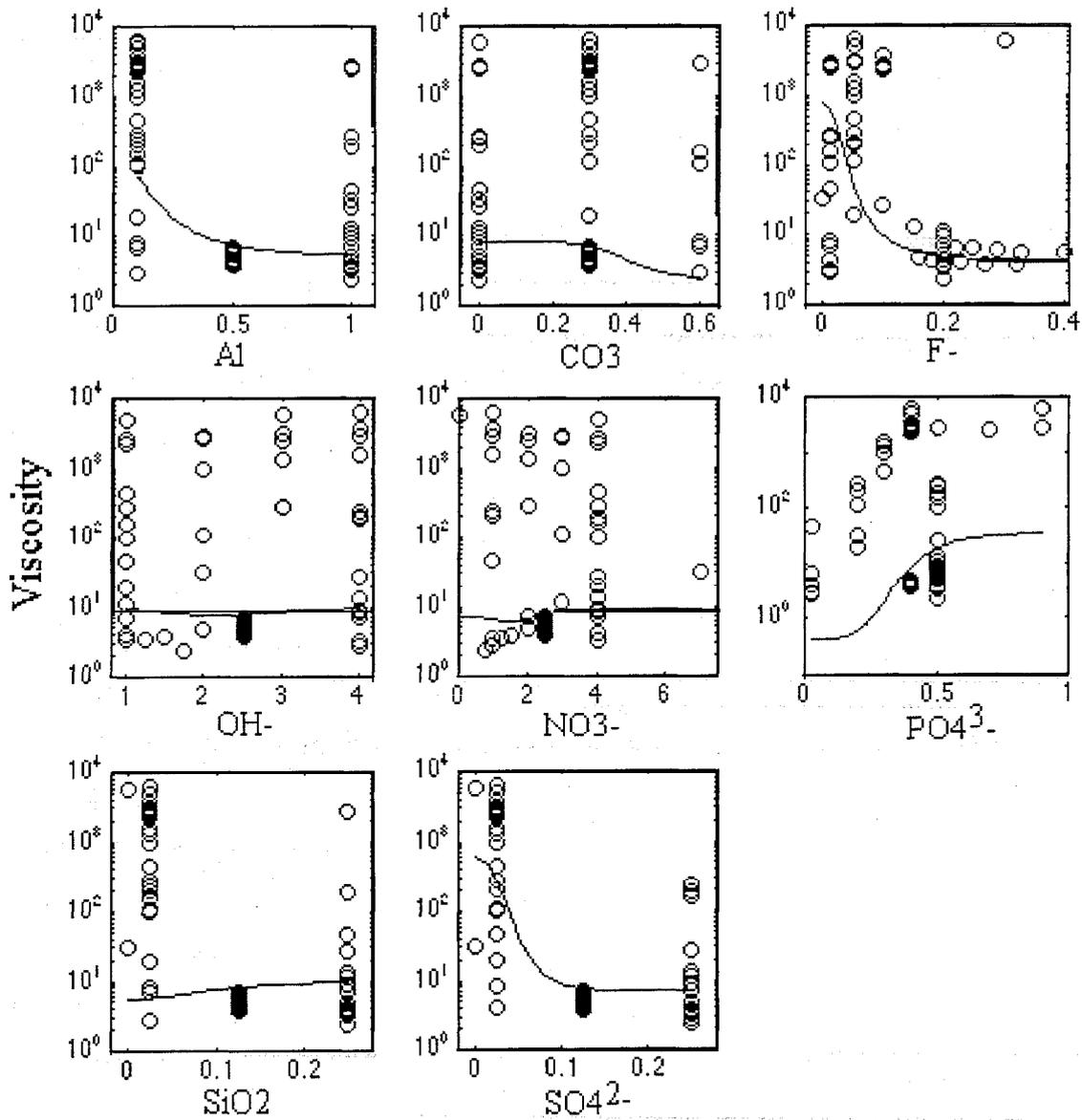
Fig. 4. Concentrations of compounds vs viscosity.

decreasing relationship between compound concentration and viscosity is evident. Fluoride and sulfate concentrations are important in the prevention of sodium phosphate plugs, while phosphate concentration is clearly important in the plug formation. Fluoride reduces the potential of a sodium phosphate plug through the formation of sodium fluoride-sod&u-n, phosphate double salt, which is called natrophosphate. While sodium phosphate forms needle-

like crystals, natrophosphate crystals are potato shaped. The role of sodium sulfate in the prevention of sodium phosphate plugs is not known, but it may also involve the formation of a double salt. Solubility tests at MSU on double salts may provide additional insights.

3.4 SUMMARY OF THE VALIDATION AND SENSITIVITY TESTS

An ANN has been adequately trained to reasonably predict the peak viscosity of Hanford simulants, which contain aluminum, carbonate, fluoride, hydroxide, nitrate, phosphate, silicate, and sulfate. The architecture of the ANN involves eight predictor variables (compounds), four hidden nodes, and a single output node (viscosity). The predictive capability of this refined ANN is demonstrated in Fig. 3. The ANN was used to determine the effect of individual chemical components on the peak viscosity of the simulants. This modeling effort confirmed several observations that were made on the effects of gradual waste cooling and simulated pump failure. First, phosphate concentration is an important variable in plug formation. Second, fluoride concentration can reduce the potential for plug formation. Third, sodium carbonate is not a primary factor in the formation of pipeline plugs even though it has been suggested that the carbonate may be responsible for the plug from tank BY-103 (Hunt et al., 2000b). Fourth, sodium hydroxide and sodium nitrate are essentially equivalent with respect to plug formation, and their primary contribution is to ionic strength. Fifth, increases in aluminum concentration appear to hinder the formation of sodium phosphate plugs less than fluoride and sulfate do, based on the magnitude of change in the scatterplots. The primary contribution of soluble aluminum is to ionic strength, while insoluble aluminum such as gibbsite would be comparable to sodium carbonate. Finally, the only significant surprise from the ANN results was the ability of sulfate to reduce the potential for plug formation.

4. SODALITE DEPOSITS IN THE SAVANNAH RIVER EVAPORATOR

4.1 BACKGROUND

The formation of the aluminosilicate mineral sodalite or its homologs has become a significant problem in the 2H evaporator at the SRS. This problem could easily spread to other

evaporators if they are used to process solutions that are laden with both silicate and aluminate in an alkaline solution. These aluminosilicates solids in the 2H evaporator have been shown to adhere tenaciously to the stainless steel surfaces inside of the evaporator system, which typically operates at approximately 120°C. The aluminosilicate deposits have led to two shutdowns of the 2H evaporator. In the first case, high-pressure water was used to clear a plugged gravity drain line. During the most recent shutdown, 1.5 M nitric acid at 90°C was used to dissolve the deposits in the evaporator pot while high-pressure water was used to remove a blocked lift line. Since the aluminum and silicon concentrations in the feed to the, 2H evaporator are not expected to change significantly in the near term, further problems with aluminosilicate deposits can be expected.

Consequently *an* investigation into which potential lixiviants or extraction agents might be able to dissolve the scale led to laboratory studies at Savannah River (Wilmarth and Fink, 1998). Nitric acid was found to work well. Since the material of construction is primarily 304 stainless steel, this oxidizing acid was desirable from a corrosion standpoint. It has been established that *strong* acids will undoubtedly dissolve aluminosilicates deposits in the evaporator. Nonoxidizing sulfuric acid and oxidizing nitric acid can also be used, but sulfuric acid is too *corrosive* (Wilmarth, 2000).

Although acids in general can be expected to dissolve aluminosilicates, the availability of data in the literature is limited somewhat *to* nonaqueous alkaline fusions directed at sample preparation prior to chemical analysis (Jackson, 1985). The use of fluoride-based molten salts is especially effective at dissolving aluminosilicates such as sodalite (Bock, 1979). However, fusion methods are not practical for use in cleaning a scale from inside process equipment. For this reason, a select group of inorganic aqueous salt solutions was chosen for the purpose of investigating their ability to dissolve a sodium nitrate/nitrite-based sodalite, which has been detected in the 2H evaporator. The primary objective of these tests was to study potential low-temperature alternatives to the hot nitric acid dissolution process. The chosen group includes compounds such as fluoride and complexing organic anions, which should aid in dissolution. A weak non-oxidizing acid and distilled water were also evaluated. The results of these dissolution tests should add to the limited amount of data available *that* addressed the dissolution of the

25

problematic sodalite. Hopefully, the number of potential choices to remove future deposits will be expanded.

The solubility of a mineral such as sodalite depends upon its preparation procedure and its thermal history. For example, the mineral may become more refractory towards dissolution in some of the selected salt solutions if it has been cured at high temperatures for a long period of time. The sodalite in these tests was prepared at a relatively low temperature of $100°C$, and the precipitate was dried at $52°C$ overnight after it was washed with distilled water. The ability of the chosen lixiviants to dissolve the sodalite was investigated at ambient temperature, which ranged between 22 and $24°C$.

4.2 SAMPLE PREPARATION AND TEST PROCEDURE

4.2.1 Simulant Solutions for the 2H Evaporator

SRS personnel have used the results of a chemical characterization at various levels inside the feed tank to the 2H evaporator to formulate the simulant used in these tests. The sodium, aluminum, and silicon concentration ranges in the feed tank were used to generate four simulant options, and the option with a total sodium concentration of 6 A4 was used in these tests. The working solution was prepared in two parts. A silicon-rich solution was prepared from sodium metasilicate pentahydrate, while the other solution contained the aluminum nitrate, sodium nitrate, and sodium nitrite. The two solutions were separately heated to $100°C$ and then combined at the start of the test to produce a final solution with the desired molar Al:Si ratio of 1. Sodium hydroxide was added to produce a solution of 4 M hydroxide when both solutions are mixed. The final concentrations of the simuiant are given in Table 8.

All solutions prepared in this work were stored in screw-top, polypropylene volumetric flasks due to their high alkalinity and never exceeded 1 L of solution. This approach minimized the potential for changes in both the salt and silicate-based solutions upon standing. Since 450 mL of solution was used in each batch, fresh solutions were prepared often.

Table 8. Composition of the reactant salt feed solution

| Species	Concentration (M)	Species	Concentration (M)
Sodium	6.05	Hydroxide	4.00
Silicon	0.05	Nitrate	1.00
Aluminum	0.05	Nitrite	1.00

4.2.2 Sodalite Preparation

The synthetic sodalite mineral was prepared in a silicon-oil-filled constant-temperature water bath, which can maintain the bath temperature within 0.25 °C of the target reaction temperature of 100°C. The bath temperature was checked periodically against a National Institute of Standards and Technology (NIST) traceable thermocouple-based meter calibrated certified through January 3, 2002. A Lightnin mixer with an electronic display of revolutions per minute (rpm) was used to stir the solutions in. the bath at 250 rpm.

The bath opening was modified with a steel plate with three openings so three reactors could be used simultaneously. Initially, two positions were used to heat the aluminum-rich and silicon-rich solutions before they were combined into the third 600-mL, stirred vessel. The reaction vessels were manufactured by Polar, Inc., and were made of polished 304 stainless steel. The vessels were straight walled with a lip, which caught the top of the plate and allowed the vessel to hang into the silicon oil. Approximately, 450 mL of the combined solution was always at or below the liquid level in the bath.

The solution was stirred using a high-density-polyethylene-coated stirrer and propeller with three 45° lobes, which turned clockwise at 250 r-pm during use. This direction of rotation forced the vessel solution downward. The shaft of the propeller passed through a close-fitting Teflon tube, which was centered in the top of a number 14 Neoprene stopper. This stopper fit snugly in the top of the reaction vessel. A 5-lb slotted hanging-scale weight of the same diameter was placed on top of the stopper to ensure that the seal with the vessel was always tight. The 47 mm-diam mixer propeller was always placed 2 cm above the bottom of the reaction vessel by aligning a mark on the mixer shaft with the opening of the chuck, and the mixer motor was

aligned with a mark on its support rod. The formation of the sodalite from its un-ionized reactants is depicted in reaction Eq. (5), which shows only nitrate as a primary anion. However, X-ray analysis indicates that both nitrate and nitrite are present in the crystal lattice:

$$6NaAlO_{2\ (aq)} + 6H_4SiO_{4\ (aq)} + 2NaNO_3 \rightarrow Na_8[\ AlSiO_4]_6\ (NO_3)_2 \bullet 4H_2O + 8H_2O\ . \qquad (5)$$
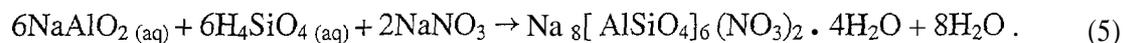
Five batch preparations were performed to produce enough sodalite for the solubility tests. The solids were washed with a large volume of distilled water to remove excess electrolyte. The solid was then placed in a drying oven set at 52°C to dry to a constant weight. This drying process usually required 12 h since the sodalite was sand-like in appearance and dried quickly. The sodalite was then sealed from the air in a plastic vessel until it was needed.

4.2.3 Sodalite Characterization

The sodalite product for the solubiiity tests was characterized in two ways: by X-ray diffraction (XRD) and by a dry screen analysis to establish the approximate particle size distribution. The results of the screen analysis of the dried and blended sodalite are presented in Table 9. United States Standard sieves were used to establish the size distribution,

An XRD spectrum of a representative sample was obtained after a sample was pulverized using an agate mortar and pestle, An XDS 2000 diffractometer from Scintag, Inc. (USA), was employed for XRD analysis. For data interpretation, the Jade 6 XRD pattern processing software from Materials Data, Inc., was used to identify peaks over a 2-theta range of 4 to 40" at a continuous scan rate of 1°/min. The XRD spectrum for this sample presented in Fig. 5 shows that the product is a well-crystallized sodium nitrate/nitrite-based sodaiite.

Table 9. Particle size distribution of the dried sodalite in the solubility tests

| Size range (μm)	Weight percent
63-74	83
53-64	14
44-53	3
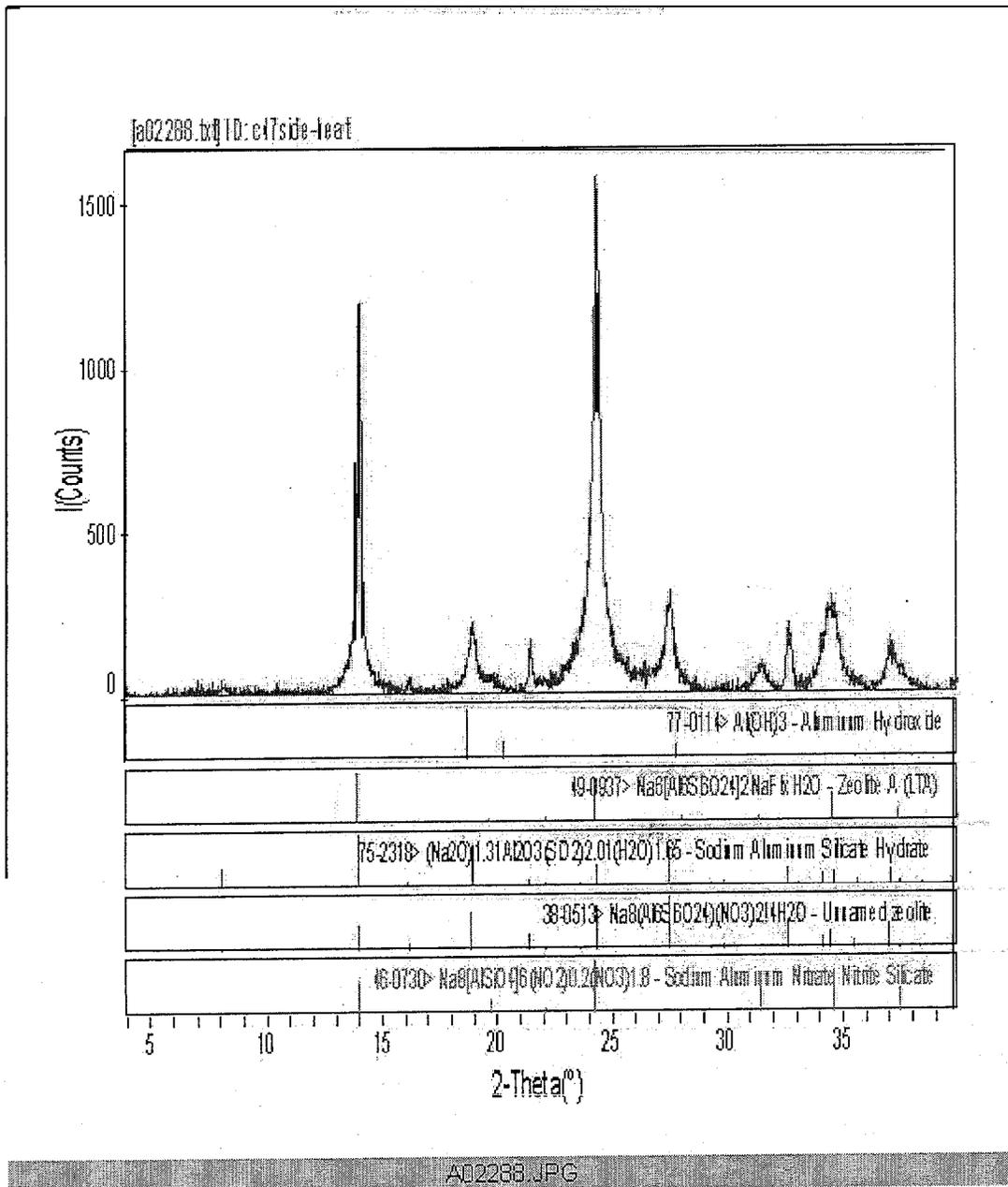
Fig. 5. X-ray diffraction spectrum of sodium nitrate/nitrite–based sodalite.

4.2.4 Lixiviants Tested

The group of possible lixiviant solutions for the sodalite was comprised of seven salts and
a weak acid. Distilled water was used as a reference. For the salt tests, the concentration was

29

maintained considerably below the salt's maximum solubility in water. An arbitrary concentration of 10% was chosen for the acetic acid solution. The lixiviant concentrations for these tests and the solubility of lixiviant in water are presented in Table 10.

4.2.5 Solubility Test Apparatus and Procedure

The solubility tests were performed using 50-mL plastic centrifuge tubes with screw-on caps. Each tube initially received 1.0 g of sodalite and 45 g of distilled water along with the mass of the desired salt to produce the concentrations of lixiviant as shown in Table 10. In the test with acetic acid, a 10% solution (based upon volume) was prepared, and 45 g of this solution was added to the centrifuge tube along with the sodalite sample.

Once each-tube had been prepared, it was sealed and placed on a rocking shaker table known as a Labquake Shaker@. The rocking of the table continued the full test duration while observations confirmed that some sodalite was always available and exposed to the lixiviant.

Table 10. Lixiviant salt solutions and concentrations

Salt or solution	Formula	Solubility in water (g/1000 g)	Concentration in tests (g/L)
Acetic acid	$C_2H_4O_2$	Very high	10% by volume
Ammonium fluoride	NH_4F	8200 at 20°C	222.4
Ammonium oxalate	$(NH_4)_2C_2O_4 \cdot H_2O$	51 at 20°C	25.5
Citric acid	$C_6H_8O_7$	100 at 25°C	50.0
Distilled water	H_2O	-----	-----
Maleic acid	$C_4H_4O_4$	790 at 25°C	111.1
Oxalic acid	$C_2H_2O_4 \cdot 2H_2O$	100 at 25°C	50.0
Sodium citrate	$Na_3C_6H_5O_7 \cdot 2H_2O$	720 at 25°C	222.2
Sodium fluoride	NaF	42 at 25°C	21.0

When the sodalite was completely dissolved, additional l-g samples of sodalite were added until no more sodalite could be dissolved. The oxalic acid test required a total of 2 g of sodalite. The citric acid, maleic acid and acetic acid required a total addition of 3 g of sodalite over a total of 21 days of operation at ambient temperature ranging between 22 and 24°C.

Solution associated with each tube was removed after 7 and 21 days for chemical analysis. Solution was removed using a 20-mL syringe connected to a 0.2-μm nylon filter. Solution was then analyzed using inductively coupled plasma (ICP). The pH of the solution was checked using pH test strip papers at the end of the test period. In other simulant tests for Savannah River (Mattus et al., 2001), the ICP analysis of aluminum was more accurate and reliable than the silicon analysis. Therefore, when the difference in concentrations was less than 10%, aluminum results were used to calculate solubilities based upon the average concentration of two analyses over 21 days.

4.3 SOLUBILITY OF SODALITE IN THE LIXIVIANTS

The results of the sodalite solubility tests are presented in Table 11. The sodalite solubility was in excess of 5.5 g per 100 g of solution in the tests with'the acetic acid solution and the weak acid salts, which included citric acid and maleic acid. Another weak acid salt, oxalic acid, was able to solubilize 3.5 g of sodalite per 100 g of solution. The pH values of the weak acid salts are usually in the range of 3 to 6. In sharp contrast, sodalite solubility for the other compounds was on the order of 0.002 g per' 100 g of solution, which was lower than the solubility of sodalite in distilled water.

The superior performance of the weak acid salts can be attributed to two factors. Under mildly acidic conditions, the aluminum cations of sodalite are exchanged with the protons while the oxalate, citrate, malate, and acetate anions are well known to complex the aluminum cation to facilitate its solubilization. The high sodalite solubility requires the presence of both factors, which are a complexing agent and a mildly acid solution. For example, citrate is a good complexing agent for aluminum, but sodalite was essentially insoluble in sodium citrate. Similarly, a high sodalite solubility would have been observed in the fluoride tests if the solutions were acidic. The acidic salts produced insoluble silicic acid gel during the

Table 11. Sodalite solubility in the lixiviant salts or solutions

Lixiviant salt or solution	Sodalite solubility (g/100 g of solution)	K_{sp} M^2/L^2
Acetic acid	5.52	9.10 E-2
Ammonium fluoride	0.002	2.50 E-l 1
Ammonium oxalate	0.002	2.50 E-l 1
Citric acid	5.73	9.87 E-2
Distilled water	0.004	1.00 E-10
Maleic acid	5.76	9.96 E-2
Oxalic acid	3.52	3.72 E-2
Sodium citrate	0.002	2.50 E-l 1
Sodium fluoride	0.002	2.50 E-l 1

solubilization of the sodalite. This silicic acid gel is expected to be present below a pH of 9. In contrast, aluminum is amphoteric and soluble in both alkaline and acid solution with a minimum, solubility near a pH of 5. The gel does not appear to halt or interfere with sodalite solubilization. It should be noted that organic-based salts should be used only after the supematant, which has a high concentration of sodium nitrate, has been removed from the evaporator. Nitrate, which is a strong oxidizing agent, would be expected to react with the organic based salts. As expected, the fluoride-based salts did not enhance sodalite solubility due to the presence of the fluoride ion. Finally, it should be noted that the K_{sp} values in these tests were considerably different from the typical K_{sp} value of 1 E-4 M^2/L^2 for sodalite in the SRS supematant simulants.

4.4 VIABILITY OF THE LIXIVIANTS

The ability of the lixiviant solutions to dissolve the sodium-based sodalite was enhanced when an exchangeable proton from the organic salt or acid was present in combination with an aluminum-complexing agent. Geochemically, this observation often occurs in nature. Many minerals can be dissolved because an acidic proton is so much smaller than sodium. The acidic proton will replace sodium cation in the crystal lattice, which can lead to a destabilization of the

solid (Garrels and Christ, 1965). If the sodalite crystal is in a solution that is below a pH value of 9.5, the oxygens of the silicate groups will be protonated and formed a silicic acid gel (pK_{a1} = 9.5). Silicic gel was produced as a by-product in four of the samples. The use of nitric acid at the SRS was also shown to react to form the silicic acid gel and acid soluble aluminum nitrate. For the acidic lixiviants, the dissolution reaction attained an equilibrium that was partly an acid/base reaction. Therefore the addition of more acid or the acid salts up to their maximum solubility would have meant that a larger mass of the sodalite mineral could have been solubilized.

Aluminum is soluble under both acidic and basic conditions; therefore, it said to be amphoteric. In the absence of complexing agents, the minimum solubility of aluminum occurs in the pH range of 4 to 5 (Lingage, 1966). Research at Savannah River has clearly shown that aluminum solubility is enhanced by the presence of oxalate (Wilmarth et al., 1997). In this current study, the organic anions associated with acetate, maleate, citrate and oxalate may therefore facilitate stabilization of aluminum in solution while their acidity is neutralized during the formation of silica-based gel.

In addition to the use of acid salts with complexing anions to aid in the dissolution of sodalite, the utility of fluoride anions was also investigated in these dilute aqueous solutions. Fluoride can form soluble complexes with silicate derivatives. Only ammonium fluoride and sodium fluorides were investigated. The ammonium salt acts as a very weak acid; it protonates the sodalite and then releases ammonia gas. Because of their corrosive nature, very acidic fluorides in a strong acid were not studied. The use of the very acidic sodium bifluoride ($NaHF_2$) salt was considered for this evaluation but was rejected due to expected high corrosivity during field use. The solubility of sodium bifluoride is approximately 32 g/L and will produce a solution with a pH of 1.

It should also be noted that the sodalite in these tests was heated only to a very low temperature of 52°C during drying. Therefore, the sodalite did not have an opportunity to become refractory towards dissolution. Deposits on tank walls or inside lines may similarly have a history of low temperature during their aging process. Therefore, the actual deposits in the evaporator may also be more amenable to a wider selection of lixiviant systems.

33

In conclusion, the dissolution results with acetic acid solution, citric acid, and maleic acid indicate that they and other lixiviant systems should be considered as low-temperature alternatives for the removal of sodalite deposits at the SRS. The primary concern with the use of these lixiviant systems is the addition of organic salts or acids to a nitrate-rich waste stream. This concern would be reduced during the neutralization process. As part of the nitric acid dissolution process, the 1.5 A4 nitric acid must be neutralized with sodium hydroxide. This ensures that the final pH of the dissolution solution is greater than 14, which will limit corrosion of the carbon steel storage tanks. Since the lixiviant solutions are only weakly acidic, the sodium hydroxide addition can be cut by more than half. It should be noted that sodium typically determines the amount of low-active grout or sandstone to be produced.

5. INITIAL STUDIES ON THE EVAPORATOR DEPOSITS AT SAVNNAH RIVER

5.1 SIMPLE SIMULANT

Prior to the development of the SRS-approved simulant in Table 8, ORNL researchers conducted preliminary tests on a comparable simulant. Each simulant was prepared from a stock solution, which was comprised of 2.2 m sodium hydroxide, 2.2 m sodium nitrate, and 1.2 m sodium chloride. It should be noted that sodium chloride was used as a substitute for sodium nitrite because of safety concerns. If the sodium nitrite was added to a solution with excess caustic before the aluminum nitrate was completely dissolved, poisonous nitrogen dioxide could be generated. In addition, it was anticipated that the sodium chloride would facilitate the formation of sodalite, which normally contains sodium chloride. Aluminum in the form of gibbsite and silicon in the form of silicic acid were **added** to separate portions of the stock solution. Aluminum and silicon concentrations were maintained within ranges from 0.5 to 1.9 m in order to produce a considerable amount of solids in a short time period. The aluminum and silicon solutions were preheated to ensure that significant amounts of soluble aluminum and silicon would be present when the samples were combined.

5.2 FORMATION OF HYDROXYSODALITE

Upon mixing, the color of the solutions changed immediately from colorless to white. After 24 h at 75–80°C, a thin layer of hard solids was observed at the interface between the colorless solution and the solids. During the next 48 h, the amount of hard deposits increased significantly as the volume of colorless solution above the deposits increased. The hard deposits did not change noticeably with additional time, even though aluminosilicates tend to change to more dense forms with time. A small portion of the hard deposits was removed for XRD analysis. The simulated deposits were comprised of hydroxysodalite, gibbsite, and faujasite. Hydroxysodalite and sodalite are in the same aluminosilicate family. One of the significant differences between the aluminosilicates is that hydroxysodalite contains sodium hydroxide while sodalite from the SRS simulant contains sodium nitrate and sodium nitrite. A sample of the simulated deposit was digested with a mixture of nitric acid and hydrofluoric acid at 90°C. The solution from this digestion process was submitted for ICP analysis. The major analytes in the deposits were aluminum, silicon, and sodium, with a trace amount of calcium. A comparison of the analytical results for the Oak Ridge and Savannah River simulants indicates that the simulants are comparable.

Additional formation tests indicated that the hard deposits could be produced with and without mixing at 100 rpm. Unfortunately, these tests were not designed to accurately determine the amount of deposits. However, another ORNL study has demonstrated that the mixing can play an important role in the amount of deposits from the Savannah River-provided simulant (Hu et al., 2001). Other formation tests in this current effort evaluated the effects of temperature. Samples with equal concentrations of aluminum and silicon were prepared, using concentrations of 0.6 and 0.8 *m*. The samples were mixed and stored at room temperature. After 144 h, no hard deposits were detected in the samples. The samples were then heated in an oven at 75–80°C. After 72 h at the elevated temperature, a large amount of hard deposits was observed in both samples. These tests clearly indicate that a minimum temperature is needed in the formation of the hard deposits. Additional tests were performed to determine the minimum temperature for the Oak Ridge simulant. This minimum temperature, should be above the temperature in the feed tank, which is normally between 30 and 40°C. Three samples with aluminum and silicon

concentrations of 1 .O m were prepared. The first sample was stored at room temperature. After 4 weeks, no hard deposits were observed in the sample. The second sample was placed in an oven at 50°C for 3 weeks, and no layers of hard deposits at the interface of the clear solution were detected. The third sample was placed in an oven at 60°C. While no hard deposits were observed after 3 days at 60 °C, deposits were detected after 7 days at 60°C. Therefore, the minimum temperature for the formation of hard deposits with this simulant must be between 50 and 60°C.

5.3 NITRIC ACID DISSOLUTION OF THE HYDROXYSODALITE

53.1 Evaporator Pot

Operators at the Savannah River tank farm used 1.5 M nitric acid at 90°C to remove the deposits from the pot of the evaporator system. A series of tests was conducted to determine the effectiveness of the nitric acid dissoiution on the simulated hard deposits. Each sample contained approximately 0.13 g of simulated hard deposits from previous solids formation tests with 1 .O m aluminum and 1 .O m silicon. In some cases, the deposits were ground into a powder to increase the available surface area, which should be comparable to the surface area in the tests with actual deposits. In contrast, other samples contained a single piece of the simulated deposit in order to minimize the available surface area, which should be comparable to the available surface area during full-scale remediation. Each sample contained 10.4 mL of 1.5 M nitric acid. This solid-to-liquid ratio was selected so that direct comparison with tests on actual evaporator deposits could be made. The addition of the nitric acid produced an appreciable amount of gas bubbles, which were probably caused by chlorine gas. 'Therefore, the sample tubes would be opened only in a partially closed fume hood. The samples were then placed in a shaker water bath or an oven at 80°C. Within 4 h, a layer of gel had surrounded the solid in the low-surface-area tests. The thickness of the gel layer ranged from 1 to 5 mm. In sharp contrast, the samples with high surface area did not generate a detectable gel layer. However, most of the fine particles could not be easily separated through agitation. At the conclusion of each test, a portion of the dissolution solution was decanted, and some of the samples were filtered through a 0.25-μm

syringe filter. The solutions were then analyzed with ICP. The aluminum concentrations for the samples with and without gel were the same: 1200 mg/L with 0.25-μm filtration and 1600 mg/L with no filtration. These results indicate that the gel does not affect the dissolution of the aluminum and that the acid dissolution process produces a considerable amount of suspended solids. With 0.25-μm filtration, the silicon concentrations were 700 and 1400 g/mL with 5 mm of gel and no detectable gel, respectively. The silicon concentrations with no filtration ranged from 1400 to 1900 g/mL. These results indicate that the gel is primarily silicon as expected.

After the liquid sample for the ICP analysis was obtained, the remainder of the liquid was decanted. If the gel thickness was 1 mm or less, the solids were permitted to dry at 80°C. The weight of the dried solids was measured to determine the effectiveness of the dissolution process. The 1.5 M nitric acid dissolution removed 69-71% of the simulated deposits. In tests with actual deposits, 1.5 M nitric acid dissolved 80−90% of the deposits from the evaporator gravity drain line (Wilmarth et al., 1997) while the same dissolution process only dissolved 59% of deposits from the evaporator pot (Wilmarth et al., 2000). A comparison of the dissolution results confirms that the Oak Ridge simulant formulation was satisfactory. In addition, these dissolution results indicate that the performance of the acid dissolution process will be sensitive to the exact chemical compounds in the deposits and their relative amounts. Other key variables may include available surface area and solid-to-liquid ratio. These results indicated that the evaporator deposits can be removed through acid dissolution with 1.5 it4 nitric acid. However, the formation of gel during the remediation effort is expected. It should be noted that a gel was formed during the successful full-scale acid dissolution of the deposits in the 2H evaporator.

5.3.2   Lift Line and Gravity Drain Line

Several factors reduce the probably that acid dissolution could be successfully used to remove the pipeline plug. In comparison with the deposits in the pot, the exposed surface area of the deposits in the line would be significantly smaller, and the free space in the line severely limits the liquid-to-solid ratio that could be employed. In addition, the lack of adequate mixing would significantly slow the kinetics of the nitric acid dissolution. The simulated hard deposits in a plastic test tube were used to represent the plugged lift line. The deposits from the test with

initial concentrations of 0.9 *m* aluminum and 0.9 *m* silicon were selected for the dissolution test. After the caustic solution on top of the hard deposits was decanted, the solids were washed with distilled water. It should be noted that an unknown amount of caustic solution was trapped in this simulated pipeline plug. After the wash solution was removed, the weight of the wet solids was determined to be approximately 3.2 g, and the height of the deposits was 23 mm. Then, 10 mL of 1.5 *M* nitric acid was added to the deposits, and the sample was placed in an oven at 85-90 "C. No changes in the height or the appearance of the simulated pipeline plug were observed after 5 days. However, a layer of gel appeared on the top layer of the simulated deposit after 9 days. The total thickness of the gel layer was 3.5 cm. Approximately 1 cm of the gel was firmly attached to the deposits, while the remainder of the gel could be easily suspended into the nitric acid solution. After 17 days, the simulated pipeline plug separated into three distinct sections. This observation suggests that the nitric acid was able to penetrate the top layer of the deposits. No further changes in the deposits were observed during the next 6 days. At the conclusion of the test, the weights of the wet solids with and without gel were 3.2 and 2.9 g, respectively. Therefore, the acid dissolution removed approximately 9% of the simulated pipeline plug after the gel was removed. In addition, the acid dissolution did not produce noticeable change in the hardness of the deposits. These results clearly support the decisions of the Savannah River tank farm operators to physically remove the plugs in the lift line and the gravity drain line with high-pressure water.

6. SODIUM NITRATE PLUG AT SAVANNAH RIVER

In February of 2001, the transfer iine from Savannah River tank 32 to the 3H evaporator system became plugged. The transfer line is 400 ft long with a diameter of 2 in. The specific gravity and temperature of the tank 32 supernatant were 1.48 g/mL and 57°C, respectively. SRS personnel provided the concentrations of the major components in the tank 32 supernatant, which consisted of 4.1 *M* sodium hydroxide, 2.5 *M* sodium nitrate, and 1.2 *M* sodium nitrate. At MSU, ESP calculations on this formulation indicated that the specific gravity would be 1.25 g/mL at 57°C. In addition, ESP predicted that no solids would appear, even if the temperature was

reduced to 20°C. The ESP predictions were confirmed through experimental studies at ORNL. If the solution was evaporated, then the first solid to appear would be sodium nitrate. If 60% of the water was evaporated and the solution was cooled to 40°C, then sodium nitrite would also be precipitated. Previously, the staff members at Savannah River tank farm had been concerned with sodium hydroxide precipitation.

Since the specific gravity for the simple formulation was much lower than the actual specific gravity in tank 32, sodium aluminate was added to the simple formulation. The ESP predicts that the saturation point for the aluminate is between 5.3 and 5.4 M. The specific gravity for the simple formulation with aluminate was 1.43 g/m&. With this more concentrated solution, the sodium nitrate precipitation would occur between 45 and 35°C without the need for evaporation. Therefore, the blockage was must likely due to sodium nitrate. Since the aluminum concentrations rarely exceed 1 M, it was recommended that water be used in the effort to remove the plug. It should be noted that additional information about the composition of the tank 32 supernatant was received after the effort was completed. In April of 2001, the tank 32 supernatant consisted of 2.6 M hydroxide, 1.5 M nitrate, 1 .1 M nitrite, 0.8 M aluminate, 0.05 M potassium, 0.03 M carbonate, 0.02 M sulfate, 0.007 M chloride, 0.007 M phosphate, 0.006 M oxalate, and 0.005 M fluoride. The specific gravity of the supematant was 1.45 g/mL.

In an effort to remove the sodium nitrate plug, personnel at the Savannah River tank farm pressurized the transfer line to approximately 340 psig with no success. Next, they placed 15-psig steam in the jacket of the transfer line prior to and during the application of 340 psig of pressure. However, the plug was apparently unaffected. Finally, the tank farm operators disconnected the transfer, line from the feed pump. When the line was separated from the pump and the isolation valve at the evaporator was opened, the liquid was abie to drain out of the transfer line. Therefore, the location of the plug was determined to be the discharge line of the feed pump. This line was flushed with cold water and then hot water. After the line was reconnected, the transfer system was flushed with hot water, and the plug was easily flushed out. A sodium nitrate plug should be easy to remove if a sufficient quantity of water has access to it. The SRS has modified its tank farm procedures in an effort to prevent similar problems in the future. Whenever the feed pump is shut down, the transfer line must now be flushed out.

7. ACKNOWLEDGMENTS,

8. REFERENCES

Bishop, *C.* M. 1995. *Neural Networks for Pattern Recognition,* Oxford University Press, New York, New York.

Bock, R. 1979. *A Handbook of Decomposition Methods in Analytical Chemistry,* John Wiley and Sons, New York, New York.

Boistelle, R., and J. P. Astier. 1988. "Crystallization Mechanisms in Solution," *J. Cryst. Growth* 90, 14.

Boley, C. S., M. C. Thompson, and W. R. Wilmarth. *2000. Technical Basis for the 242-16H Evaporator Cleaning Flowsheet,* WSRTC-TR-2000-00211, Westinghouse Savannah River Company, Aiken, South Carolina.

Garrels, R. M., and C. L. Christ; 1965. *Solutions, Minerals and Equilibria,* Freeman, Cooper & Company, San Francisco, Caiifomia.

Herting, D. L. 1999. "U-Farm Cooling Test Results, Final Report," Numatec Hanford Corporation Internal Memo #82800-99-039, Richland, Washington.

Herting, D. L. *2000. Saltcake Dissolution FY* 2000 *Status Report,* HNF-7031, Fluor Hanford, Richland, Washington.

Herting, D. L. 2001. *Saltcake Dissolution FY 2001 Status Report,* HNF-8849, Fluor Hanford, Richland, Washington.

Homik, K., M. Stinchcombe, and H. White. 1989. "Multilayer Feedforward Networks Are Universal Approximators," *Neural Networks 2,359.*

Hu, M .Z., D. W. DePaoli, and D. T. Bostick. 2001. *Dynamic Particle Growth Testing: Phase I Studies,* ORNL/TM-2001/100, Oak Ridge National Laboratory, Oak Ridge, Tennessee.

Hunt, R. D., T. A. Dillow, J. R. Parrott, Jr., J. C. Schryver, C. F. Weber, and T. D. Welch. 2000a. *Waste Preparation and Transport Chemistry: Results of the FY 2000 Studies,* ORNL/TM-2000/298, Oak Ridge National Laboratory, Oak Ridge, Tennessee.

Hunt, R. D., C. P. McGinnis, C. F. Weber, T. D. Welch, and J. R. Jewett. 2000b. *FY 2000 Saltcake Dissolution and Feed Stability Workshop,* ORNL/TM-2000/202, Oak Ridge National Laboratory, Oak Ridge, Tennessee.

Hunt, R. D., E. C. Beahm, C. W. Chase, J. L. Collins, T. A. Dillow, and C. F. Weber. 1999. *Prevention of Solids Formation: Results of the FY 1999 Studies,* ORNL/TM-1999/263, Oak Ridge National Laboratory, Oak Ridge, Tennessee.

Jackson, M. L. 1985. *Soil Chemical Analysts-Advanced Course,* 2nd ed., published by the author, Madison, Wisconsin.

Jain, A. K., J. Mao, and K .M. Mohiuddin. 1996. "Artificial Neural Networks: A Tutorial," *Computer* **29,** 3 1.

Kelly, M. G., and B. M. Mauss. 1986. *Viscosity Study-Prediction of Electrolytic Solutions and Slurries,* SD-WM-TI-222, Rockwell Hanford Operations, Hanford, Washington.

Lee, D. D., and J. L. Collins. 2001. *Evaluation of the Small Tank Tetraphenylborate Process Using a Bench-Scale 20-L; Continuous Stirred Tank Reactor System at Oak Ridge National Laboratory, Results of Test 5,* ORNL/TM-2001/42, Oak Ridge National Laboratory, Oak Ridge, Tennessee.

Leonard, R. A., S. B. Aase, H. A. Arafat, D. B. Chamberlain, C. Conner, M. C. Regalbuto, and G. F. Vandegrift. 2001. *Interim Report on a Multi-Day Test of the Caustic-Side Solvent Extraction Flowsheet for Cesium Removal from a Simulated SRS Tank Waste,* ANL-01/10, Argonne National Laboratory, Argonne, Illinois.

Lingane, J. J. 1966. *Analytical Chemistry of Selected Metallic Elements,* Reinhold Publishing Corporation, New York, New York.

Iinke, W. F. 1965. *Solubilities,* 4th ed., American Chemical Society, Washington, D.C.

Lippmann, R. P. 1987. "An Introduction to Computing with Neural Nets," *ZEEE ASSP Mag.*, **4**(2):4.

Mattus, A. J., C. H. Mattus, and R. D. Hunt. 2001. *Kinetic Testing of Nitrate-Based Sodalite Formation over the Temperature Range of 40 to ZOO °C*, ORNL/TM-2001/117, Oak Ridge National Laboratory, Oak Ridge, Tennessee.

Nyman, M. D., T. J. Headley, T. M. Nenoff, and L. D. Bustard. 2001. *Performance of IE-911: Characterization of As-Received, NaOH-treated and Simulant-treated CST,* SAND2001 -0435P, Sandia National Laboratories, Albuquerque, New Mexico.

Spencer, B. B., K. K. Anderson, H. L. Jennings, T. E. Kent, P. A. Taylor, and M. W. Geeting. *2001. Evaluation of Gas Disengaging Equipment Supporting a Crystalline Silicotitanate Ion-Exchange Column System,* ORNL/TM-2001/46, Oak Ridge National Laboratory, Oak Ridge, Tennessee.

Taylor, P. A., and C. H. Mattus. *2001. Thermal and Chemical Stability of Baseline and Zmproved Crystalline Silicotitanate,* ORNL/TM-2001/165, Oak Ridge National Laboratory, Oak Ridge, Tennessee.

Toghiani, B., and J. S. Lindner. 2001. *DIAL/MSU Saltcake Dissolution: Fiscal Year 2000 Status Report,* TR 00-l Tanks Focus.

Weber, C. F., E. C. Beahm, and J. S. Watson. 1999. "Modeling Thermodynamics and Phase Equilibria for Aqueous Solutions of Trisodium Phosphate," *J. Solution Chem. 28,* 1207.

Welch, T. D., K.K. Anderson, D. T. Bostick, T. A. Dillow, M. W. Geeting, R. D. Hunt, R. Lenarduzzi, A. J. Mattus, P. A. Taylor, and W. Wilmarth. *2000. Hydraulic Performance and Gas Behavior of a Tall, Crystalline-Silicotitanate Zon-Exchange Column,* ORNL/TM-1999/103, Oak Ridge National Laboratory, Oak Ridge, Tennessee.

Welch, T. D. 2001. *Tank Waste Transport Stability: Status Summary of Slurry and Salt-Solution Studiesfor FYOI,* ORNUTM-2001097, Oak Ridge National Laboratory, Oak Ridge, Tennessee.

Wilmarth, W. R. *2000. Comparison of Nitric Acid and Sulfuric Acid Dissolution of Samples from the 242-16H Evaporator Pot,* WSRTC-TR-2000-00209, Westinghouse Savannah River Company, Aiken, South Carolina.

Wilmarth, W. R., C. J. Coleman, A. R. Jurgensen, W. M. Smith, J. C. Hart, W. T. Boyce, D. Missmer, and *C.* M. Conley. *2000. Characterization and Dissolution Studies of Samples from the 242-16H Evaporator,* WSRC-TR-2000-00038, Westinghouse Savannah River Company, Aiken, South Carolina.

Wilmarth, W. R., and R. A. Peterson. *2000. Analyses of Surface and Variable Depth Samples from Tank 43H*, WSRS-TR-2000-00208, Westinghouse Savannah River Company, Aiken, South Carolina.

Wilmarth, W. R., and S. D. Fink. *1998. Evaporator Cleaning Studies,* WSRTC-TR-98-00406, Westinghouse Savannah River Company, Aiken, South Carolina.

Wilmarth, W. R., S. D. Fink, D. T. Hobbs, and M. *S.* Hay. 1997. *Characterization and Dissolution Studies of Samples from the 242-l 6H Evaporator Gravity Drain Line,* WSRC-TR-97-0326, Westinghouse Savannah River Company, Aiken, South Carolina.

INTERNAL DISTRIBUTION

1. J. N. Herndon		9. J. C. Schryver
2-5. R. D. Hunt		10. J. S. Watson
6. R. T. Jubin		11. C. F. Weber
7. L. N. Klatt		12. T. D. Welch
8. C. P. McGinnis		13. ORNL OTIC-RC

EXTERNAL DISTRIBUTION

14. Hani Al Habbash, 205 Research Boulevard, Starkville, MS 39759-9734
15. Dan Baide, CH2M Hill Hanford Group, P.O. Box 1500, MSIN S7-90, Richland, WA 99352
16. Blaine Barton, CH2M Hill Hanford Group, P.O. Box 1500, MSIN R7-11, Richland, WA 99352
17. Nidhi Bhandari, Florida International University, 10555 West Flagler Street, CEAS 2100, Miami, FL 33174
18. Brian Brendel, CH2M Hill Hanford Group, P.O. Box 1500, MSIN S7-90, Richland, WA 99352
19. Jerry Cammann, CH2M Hill Hanford Group, P.O. Box 1500, MSIN T4-08, Richland, WA 99352
20. Joe Cruz, Department of Energy, Office of River Protection, P.O. Box 550, MISN H6-60, Richland, WA 99352
21. John Garfield, Numatec Hanford Company, P.O. Box 1300, MSIN R3-73, Richland, WA 99352
22. Ken Gasper, CH2M Hill Hanford Group, P.O. Box 1500, MSIN H6-19, Richland, WA 99352
23. Tom Gutman, U.S. Department of Energy, Savannah River Operations Office, P.O. Box A, Aiken, SC 29802
24. Pete Gibbons, Numatec Hanford Company, P.O. Box 1300, MSIN K9-91, Richland, WA 99352
25. Jim Henshaw, AEA Technology, B220 Harwell, Didcot, Oxfordshire, UK, OX11 0RA
26. Dan Herting, Fluor Daniel, P.O. Box 1970, MSIN T6-07, Richland, WA 99352
27. David Hobbs, Westinghouse Savannah River Company, Savannah River Technology Center, Building 773-A, Aiken, SC 29808
28. Jim Honeyman, CH2M Hill Hanford Group, P.O. Box 1500, MSIN H6-62, Richland, WA 99352
29. James Jewett, Numatec Hanford Company, P.O. Box 1300, MSIN R3-73, Richland, WA 99352
30. Randy Kirkbride, Numatec Hanford Company, P.O. Box 1300, MSIN R3-73, Richland, WA 99352

31. Jeff Lindner, DIAL, 205 Research Boulevard, Starkville, MS 39759-9734
32. Ruben Lopez, Florida International University, 10555 West Flagler Street, CEAS 2100, Miami, FL 33 174
33. Graham MacLean, FFS, P.O. Box 1050, MSIN G3-10, Richland, WA 99352
34. Billie Mauss, Department of Energy, Office of River Protection, P.O. Box 550, MISN H6-60, Richland, WA 99352
35. Jerome Morin, Westinghouse Savannah River Company, Savannah River Technology Center, Building 703-H, Aiken, SC 29808
36. Ron Or-me, Numatec Hanford Company, P.O. Box 1300, MSIN R3-73, Richland, WA **99352**
37. John Plodinec, DIAL, 205 Research Boulevard, Starkville, MS 39759-9734
38. Wally Schulz, W2S Company, 12704 Sandia Ridge Place, NE, Albuquerque, NM 87111
39. Rajiv Srivastava, Florida International University, 10555 West Flagler Street, CEAS 2100, Miami, FL 33174
40. Walt Tamosaitis, Westinghouse Savannah River Company, Savannah River Technology Center, Building 773-A, Aiken, SC 29808
41. Tanks Focus Area Headquarters Program Lead, c/o Kurt Gerdes, DOE Office of Science and Technology, 19901 Germantown Road, 1154 Cloverleaf Building, Germantown, MD 20874-1290
42. Tanks Focus Area Program Manager, c/o T.P. Pietrok, U.S. Department of Energy, Richland Operations Office, P.O. Box 550, MSIN K8-50, Richland, WA 99352
43. Tanks Focus Area Technical Team, c/o B.J. Williams, Pacific Northwest National Laboratory, P.O. Box 999, MISN K9-69, Richland, WA 99352
44. Rex Thompson, CH2M Hill Hanford Group, P.O. Box 1500, MSIN T4-08, Richland, WA 99352
45. Becky Toghiani, Mississippi State University, School of Chemical Engineering, P.O. Box 9595, MS State, MS 39762
46. George Vandegrift, Argonne National Laboratory, Building 205, 9700 South Cass Avenue, Argonne, IL 60439
47. Bill Van Pelt, Westinghouse Savannah River Company, Savannah River Technology Center, Building 773-A, Aiken, SC 29808
48. Bill Wilmarth, Westinghouse Savannah River Company, Savannah River Technology Center, Building 773-A, Aiken, SC 29808